OPERATIONAL SCHEDULING OF POWER PLANTS WITH FLEXIBLE CARBON CAPTURE UNDER UNCERTAIN ELECTRICITY PRICES

A Thesis

by

MANALI SUNIL ZANTYE

Submitted to the Office of Graduate and Professional Studies of
Texas A&M University
in partial fulfillment of the requirements for the degree of

MASTER OF SCIENCE

Chair of Committee,	M. M. Faruque Hasan
Committee Members,	Mahmoud M. El-Halwagi
	Ying Li
Head of Department,	M. Nazmul Karim

August 2019

Major Subject: Chemical Engineering

ABSTRACT

The use of fossil fuels to meet the global energy demand has led to a significant increase in CO_2 emissions. CO_2 emissions from coal-fired power plants, in particular, constitute a major part of the global greenhouse gas (GHG) emissions. Capturing CO_2 from power plant flue gas using solvent-based absorption process is one of the most effective options of reducing emissions. However, the high energy requirement of solvent regeneration and CO_2 compression prevents widespread deployment of the technology. This can be mitigated by flexible operation of the capture process in response to dynamic variation in electricity prices. The literature in the dynamic scheduling of power plants with flexible carbon capture systems mostly assumes perfect foreknowledge of electricity prices. However, electricity markets exhibit high uncertainty in reality, and it is necessary to account for price uncertainty in optimal decision-making.

In this work, we consider a pulverized coal-fired power plant retrofitted with a carbon capture unit, which varies its load with variation in electricity price. We first pose a deterministic problem that aims to maximize profit assuming complete knowledge of prices in the day-ahead electricity market. This is then extended to incorporate price uncertainty. We apply a multi-stage stochastic programming approach to determine an optimal hourly schedule of power production and carbon capture operations, while meeting a strict regulation on CO_2 emissions. Since hourly electricity prices can assume a range of values, we need to consider a large number of price scenarios. To reduce the resulting computational complexity in the optimization framework, we develop low-complexity surrogate models for optimal action policy at each stage. These models are then used to determine total optimal profit for different real-time scenarios of electricity price. Our approach is able to obtain solutions with the expected value of perfect information under uncertainty within 25% of the maximum achievable profit, while keeping CO_2 emissions sufficiently below the threshold limit.

ACKNOWLEDGEMENTS

I would like to express heartfelt gratitude to my research advisor and committee chair, Dr. M. M. Faruque Hasan for his unwavering support during the past two years. This work would not have been possible without his invaluable advice and recommendations. I am also thankful for the guidance from my committee members, Dr. Mahmoud M. El-Halwagi and Dr. Ying Li during the course of my thesis.

Furthermore, I would like to acknowledge the support of my research colleagues, the insightful discussions I had with them went a long way in shaping the direction of my research. I am thankful to the faculty at the Department of Chemical Engineering at Texas A&M University for creating an effective learning environment. I am also grateful for help from graduate program specialists, Ashley and Terah, for making my graduate study a smooth experience. Last but not the least, I would like to thank my parents, friends and family for their unconditional love and support which has always motivated me to do my best.

CONTRIBUTORS AND FUNDING SOURCES

Contributors

This work was supported by a thesis committee consisting of Dr. M. M. Faruque Hasan and Dr. Mahmoud M. El-Halwagi of the Department of Chemical Engineering and Dr. Ying Li of the Department of Mechanical Engineering.

All other work for the thesis was completed independently by the student.

Funding Sources

This work received funding support from U.S. National Science Foundation (award number CBET-1606027).

TABLE OF CONTENTS

Page

ABSTRACT ii

ACKNOWLEDGEMENTS iii

CONTRIBUTORS AND FUNDING SOURCES iv

TABLE OF CONTENTS v

LIST OF FIGURES vii

LIST OF TABLES viii

1. INTRODUCTION 1

    1.1 Overview of Carbon Capture in Thermal Power Plants 1
    1.2 Research Goals 5
    1.3 Outline of the Thesis 5

2. BACKGROUND AND LITERATURE REVIEW 7

    2.1 Flexible Carbon Capture Exploiting Variability in Electricity Price 7
    2.2 Electricity Market Operation Mechanism 10
    2.3 Carbon Market Mechanism 11
    2.4 Research Gaps and Objectives 11

3. DETERMINISTIC SCHEDULING 13

    3.1 Model Formulation 14
    3.2 A Deterministic Case Study 18

4. MULTI-STAGE STOCHASTIC DYNAMIC OPTIMIZATION 22

    4.1 Value Iteration Algorithm 25
    4.2 Algorithm Implementation 26
        4.2.1 Backward Recursion: Obtaining Optimal Action Policy 26
            4.2.1.1 Penalty Parameter λ 29
            4.2.1.2 Approximating the Optimal Value Function and Action Policy 30
        4.2.2 Forward Simulation: Calculating Total Profit 34

5. RESULTS AND DISCUSSION 37

5.1 CO_2 Emission Intensity 37
5.2 Total Profit 39
5.3 Optimal Action Policy 41

6. CONCLUSIONS AND RECOMMENDATIONS 44

6.1 Conclusions 44
6.2 Recommendations for Future Work 45

REFERENCES 47

APPENDIX A. MODELS FOR OPTIMAL DECISION VARIABLES AND VALUE FUNCTION 55

A.1 Input Variables 55
A.2 Models for Penalty parameter of 10 55

LIST OF FIGURES

FIGURE Page

1.1 Technologies for CO_2 capture from power plants 2

1.2 Process schematic of post-combustion carbon capture with solvent-based CO_2 absorption system..... 3

1.3 ERCOT settlement point prices for two representative days in 2017..... 4

2.1 Process schematic of solvent-based post-combustion carbon capture system with solvent storage tanks for flexible operation..... 9

3.1 Optimal power plant schedule for deterministic case 19

3.2 Deterministic solution: Net CO_2 emissions profile..... 20

4.1 Two-fold approach in value iteration algorithm 28

4.2 Contour plots of optimal value function and action policies for t = 24 and t = 23 32

4.3 Backward recursion workflow..... 33

4.4 Stochasticity in electricity price 36

5.1 Variation of daily average CO_2 emission intensity: E^N_{avg} with penalty parameter 38

5.2 Variation of stochastic and deterministic profit with λ..... 39

5.3 Variation of value of perfect information (VPI) with λ 41

5.4 Hourly optimal action policy for λ = 10 and λ = 100 43

LIST OF TABLES

TABLE Page

3.1 Parameter values and variable bounds 16

3.2 Profit components in deterministic case (in $)..... 18

A.1 Input variable set (X) 55

A.2 Models for gross power g_t 55

A.3 Models for rate of CO_2 absorption $r_{A,t}$ 58

A.4 Models for rate of CO_2 desorption $r_{D,t}$ 61

A.5 Models for value function V_t 65

1. INTRODUCTION

Driven by rapid economic development, the global energy demand continues to increase. Despite the efforts of policy makers around the world in promoting renewable energy resources for sustainable consumption, the contribution of fossil fuels to meet the energy demand has remained constant at more than 80% over three decades. This has led to an unprecendented increase in worldwide CO_2 emissions, which reached a record high of 33.1 gigatonnes (Gt) in 2018[1]. Of this, coal-fired power generation alone accounted for nearly 30% of the emissions. The rise in emissions has several long-term negative consequences, including an increase in global temperatures, rise in sea levels and water scarcity[2].

The continued use of fossil fuels for electricity generation makes it necessary to invest in emission reduction efforts such as post-combustion CO_2 capture. The captured CO_2 can be injected in underground rock formations for enhanced oil recovery[3–6]. Another economical end-use of CO_2 is through conversion to various value-added fuels and chemicals[7–11]. However, despite the potential of carbon capture and storage (CCS) retrofits in coal power plants to reduce CO_2 emissions by 90%, widespread deployment of the technology remains far from reality. Currently, only nine power plants exist worldwide with large scale CCS projects[12]. Among these, the Boundary Dam CCS project in Canada and the Petra Nova Carbon Capture project in the U.S. are in operation while the others are still in early development stages. Significant energy and investment requirement in CO_2 separation, compression and transportation stages restricts commercial scale-up of the technology. CCS reduces net energy output of power plants by 25-40%[13], which translates to around 70% increase in production costs as compared to operating without a capture unit[14]. An overview of the energy-intensive CO_2 capture mechanism is presented below.

1.1 Overview of Carbon Capture in Thermal Power Plants

Based on the plant configuration, there are three main types of carbon capture methods: pre-combustion capture, post-combustion capture and oxy-fuel combustion capture[15]. Among these,

the most viable technology for large-scale carbon capture deployment in existing power plants is post-combustion capture[16]. Furthermore, there are different available technologies to separate CO_2 from post-combustion flue gas. These include physical and chemical absorption, adsorption and membrane separation[17–21]. The most promising and conventionally-used method of separation is chemical absorption, which can be further classified depending on the choice of solvent[22]. Figure 1.1 depicts the various CO_2 capture alternatives in coal power plants.

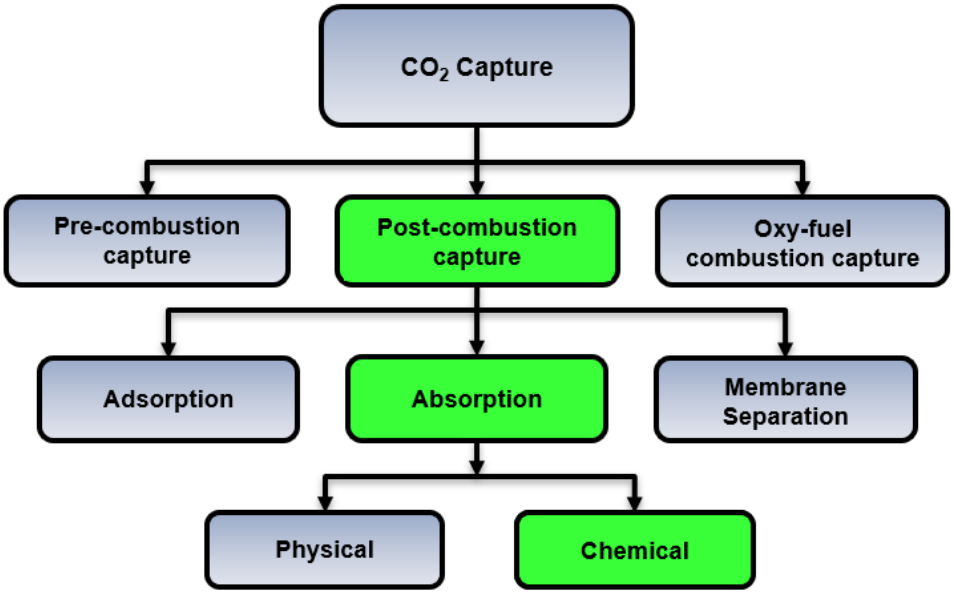

Figure 1.1: Technologies for CO_2 capture from power plants. The alternatives marked in green are the most viable ones for commercial scale-up and are considered in this work.

Commonly used solvents for chemical absorption include: i) amine-based solvents, namely monoethanolamine (MEA), diethanolamine (DEA) and triethanolamine (TEA)[23,24]; ii) ammonia[25,26]; and iii) piperazine promoted potassium carbonate (K_2CO_3)[27]. MEA is the preferred solvent due to its commercial availability and low cost. Figure 1.2 shows the overall process scheme of a power plant integrated with a solvent-based post-combustion CO_2 capture system[19]. For ease of analysis, the generation system block is shown to represent the base plant without capture. Flue gas produced on coal combustion in the boiler of the generation system is directed to the capture

system for CO_2 removal. Firstly, the flue gas enters a scrubber where it flows counter-currently with the solvent (MEA) to remove CO_2 by chemical absorption. Solvent leaving the scrubber is loaded with CO_2, and is called 'rich solvent'. This rich solvent is heated to 100-120°C in a rich-lean heat exchanger[28]. It then enters the top of a stripper where CO_2 desorption and solvent regeneration occurs. The lean solvent leaving the stripper bottom is recirculated back to the scrubber. The stream leaving the top of the stripper is high purity CO_2, which is then compressed and transported for further use in various applications such as sequestration or conversion to value-added fuels and chemicals.

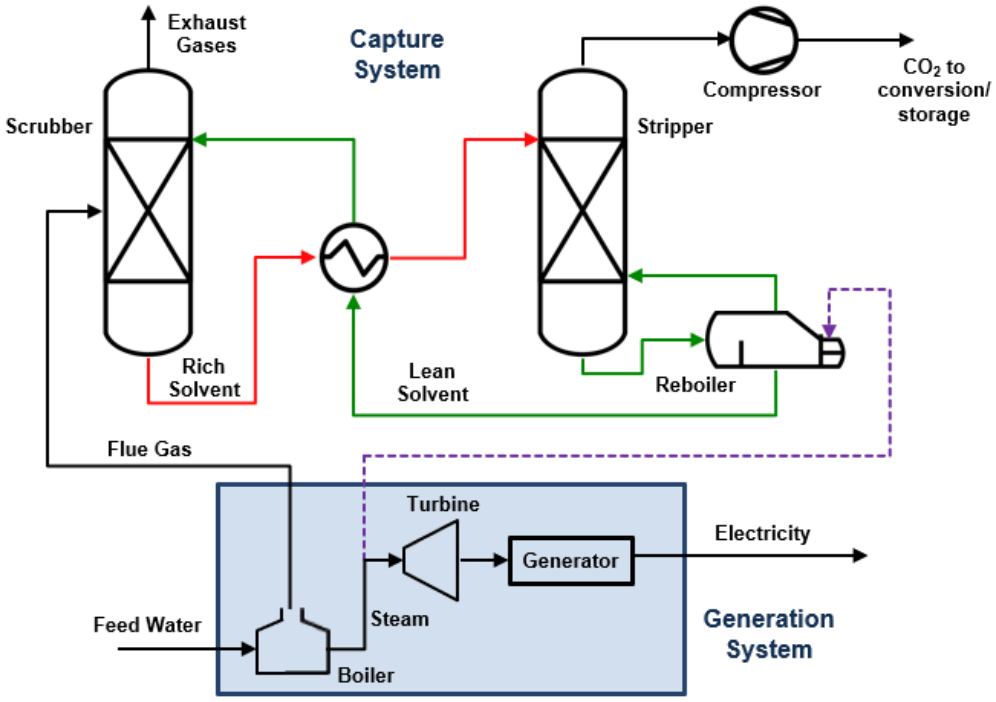

Figure 1.2: Process schematic of post-combustion carbon capture with solvent-based CO_2 absorption system.

Heat required for solvent regeneration in the stripper is supplied by steam from the reboiler. This low pressure steam requirement is typically met by the extraction of a portion of steam from intermediate and low pressure turbines of the generation system in the power plant[28–30]. This

causes a reduction in steam input to the turbines, thereby reducing the power output of the plant. Furthermore, the energy required in CO_2 compression adds to the power output reduction due to the capture system.

To offset the high energy penalty and costs associated with CO_2 capture, the dynamic variability in electricity prices can be leveraged. Owing to fluctuating electricity demand and several other market factors, real-time electricity prices exhibit high variability. Figure 1.3 depicts the electricity market prices for two representative days from 2017 for the Houston load zone of the Electric Reliability Council of Texas (ERCOT)[31].

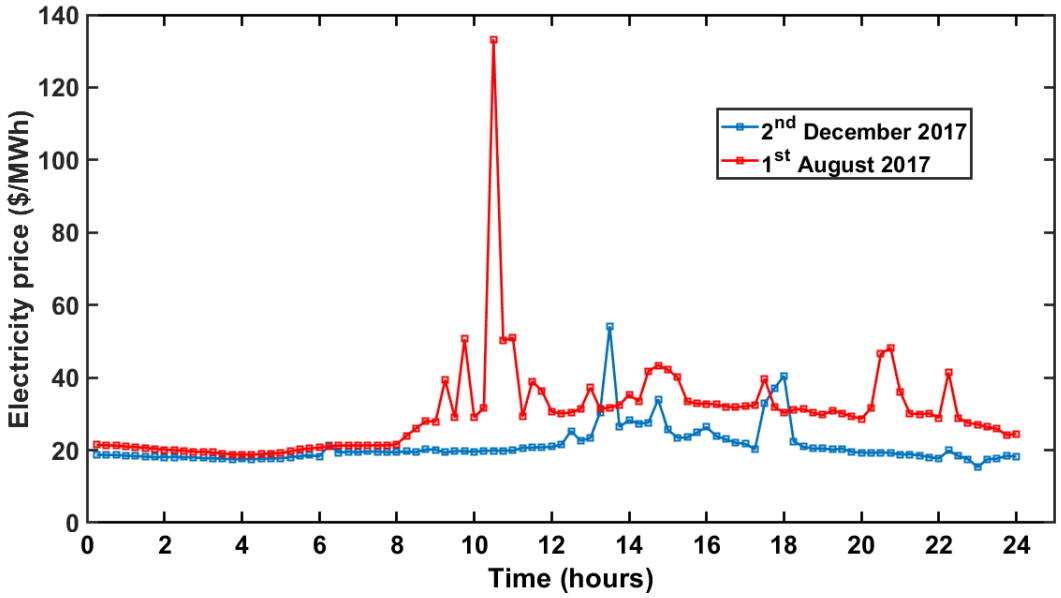

Figure 1.3: ERCOT settlement point prices for two representative days in 2017.

Figure 1.3 shows the price variation in a day of winter and a summer day in 2017. The graph is indicative of the daily and seasonal variability in real-time electricity prices. This variability can be used to vary the capture system load to make CO_2 capture more profitable.

Flexible operation of the capture system, i.e. dynamically varying its load in response to fluctuating electricity prices can make the capture system operation more profitable and suitable for

large-scale deployment as compared to the conventional operation. Among the three capture methods described in this section, post-combustion capture offers the highest feasibility of flexible operation as the capture system can be partially or completely circumvented by adjusting the solvent circulation flow[32].

1.2 Research Goals

The overarching goal of this research is to identify modifications in the conventional operation of thermal power plants with CCS retrofits to make the technology economically viable for broad uptake. We consider flexible operation of the carbon capture system leveraging volatile electricity prices to reduce its high energy penalty. Time-varying solvent storage is used to facilitate flexible operation and to minimize CO_2 venting to the atmosphere. We first analyze a deterministic case with perfect knowledge of hourly electricity price in the day-ahead price market. This model serves as a benchmark and solving it establishes an upper bound on profit. However, real-time electricity prices are highly uncertain. Therefore, the deterministic model is extended to account for price uncertainty. The resultant stochastic problem is divided into multiple stages corresponding to each hour and a stochastic programming algorithm is applied to solve for dynamic recourse.

We present a novel application of the value iteration algorithm in the optimal scheduling under uncertainty in electricity prices. The conventional value iteration algorithm is modified to ensure that the constraint on cumulative CO_2 emissions is satisfied. Due to the large number of possible price scenarios, the optimization problem is solved for a fixed set of hourly electricity prices and surrogate models are developed to estimate decisions for intermediate prices. This eliminates optimizing at each electricity price point, thereby reducing the computational complexity. Moreover, as discretization of the state space (electricity price) is avoided, it becomes possible to determine optimal profit and operation strategy for any value of electricity price between its upper and lower bounds.

1.3 Outline of the Thesis

The organization of the thesis is as follows:

Section 2 gives an overview of flexible carbon capture mechanism in thermal power plants and a comprehensive literature study of past work in improving the profitability of the technology. It also delineates the challenges which exist and our objectives to bridge the research gap through this work. Furthermore, we present a brief discussion on different aspects of the electricity and carbon markets in this section.

Section 3 presents the deterministic model of flexible carbon capture and its application to a specific case study. We also discuss the results on solving the aforementioned model and compare its solution to conventional capture system operation.

Section 4 elucidates the various approaches on incorporating uncertainty in the optimization formulation and significant past works on each approach. We also introduce the stochastic programming approach based on value iteration. We discuss different attributes of the value iteration algorithm and its application in our problem. Furthermore, we elaborate on the formulation of a stochastic model to account for price uncertainty from the deterministic model. We also present the solution strategy to solve the model along with the associated computational challenges. The approach for handling the computational complexity is discussed in this section.

Section 5 elaborates on the results of the stochastic model and their significance. The results obtained under uncertainty are compared with the deterministic model solution. The discussion of the results has been split into three parts: i) CO_2 emission intensity, ii) Total profit, and iii) Optimal action policy.

Finally, Section 6 concludes the thesis and presents a summary of the overall work with key results. Scope for future work has also been discussed in this section.

2. BACKGROUND AND LITERATURE REVIEW

A brief discussion on the flexible CO_2 capture operation in thermal power plants and its advantages is provided in this section. Furthermore, some key aspects of electricity and carbon markets have been highlighted along with relevant assumptions which would be used in further sections for model formulation. Based on the overview, we identify research gaps and outline our research goals.

2.1 Flexible Carbon Capture Exploiting Variability in Electricity Price

Previous research on post-combustion carbon capture systems is mostly focused on operating continuously at a fixed load, with all exhaust flue gas from the generation facility sent to the capture system[13,17,33–37]. This makes carbon capture less alluring due to the consumption of a large portion of electricity which could otherwise be monetized. Such inflexible operation is referred to as the 'base-case' condition in this work. The base-case condition involves the power plant operating at a fixed and steady state load where the rates of CO_2 absorption, desorption and compression in the capture system are kept equal at all times.

On the other hand, flexible operation leverages the variability in electricity prices to dynamically vary the power output and capture system load to maximize profit. Lucquiaud et al.[38] have analyzed the steam cycle operation of a dynamically operated generation system. With a turbine system conducive to dynamic operation, a power plant can vary the energy output. This also enables the base power plant to adjust the grid supply in presence of other renewable and intermittent energy sources[39].

Flexible operation allows the power plant to supply more electricity to the grid during periods of high electricity price, with little or no carbon capture. During periods of low price, the generation system can operate at the minimum load and a major portion of electricity from the generation system can be directed to the capture system. Thus, the capture system can be operated relatively independent of the generation system, reducing its 'parasitic' energy dependence and improving

the overall power plant profitability[28,39].

Previous research on flexible post-combustion carbon capture in thermal power plants investigates three primary modes of flexible operation[40–42]:

(1) Exhaust gas venting: capture system operating at partial load, or complete bypass of capture system with venting unprocessed emissions,
(2) Solvent storage: capture system operating at partial load with solvent storage to mitigate venting, and
(3) Time-varying solvent regeneration: capture system operating at partial load with rich solvent continuously recirculated to scrubber until it becomes saturated with CO_2, thus preventing additional capture.

Chalmers et al.[39] provided a comprehensive review of these modes of flexible operation. Cohen et al.[43] considered flexible power plant operation in response to daily and seasonal variations in electricity price. They analyzed the flexibility in terms of 'on' and 'off' periods of CO_2 capture, while venting the gas in periods of no capture. Lucquiaud and co-workers[44] proposed an optimal part-load operation strategy of a power plant with carbon capture using an Aspen model. However, they also considered complete bypass of the capture unit during periods of no capture.

The major motivation behind employing ancillary facilities like solvent storage is when there are environmental regulations restricting the amount of CO_2 emissions. Specifically, in cases where there is a penalty on CO_2 emissions or a CO_2 price as in a cap-and-trade carbon market, it would be economically beneficial for the power plant to store the CO_2 from absorption at periods of peak electricity demand/price using solvent storage[45]. The CO_2 rich solvent would later be regenerated when the electricity price is low.

The solvent storage mode of flexible capture system operation is the most explored one. Chalmers et al.[46] focused on part-load steady-state operation of a power plant with flexible carbon capture. They developed a model to study the economic benefits for scenarios of both venting CO_2 and solvent storage. Zaman et al.[47] optimized the operational variables for time-varying solvent regeneration and solvent-storage modes in gPROMS. The optimization is done for a 24 hour time period

with varying electricity price and a penalty on CO_2 emissions. Patino-Echeverri and co-workers[48] determined that solvent storage could be cost-effective for power plants in areas with high variance of electricity prices, justifying the capital investment for storage tanks. Figure 2.1 depicts the modifications to the power plant process scheme to enable flexible carbon capture, facilitated by solvent storage and a venting system.

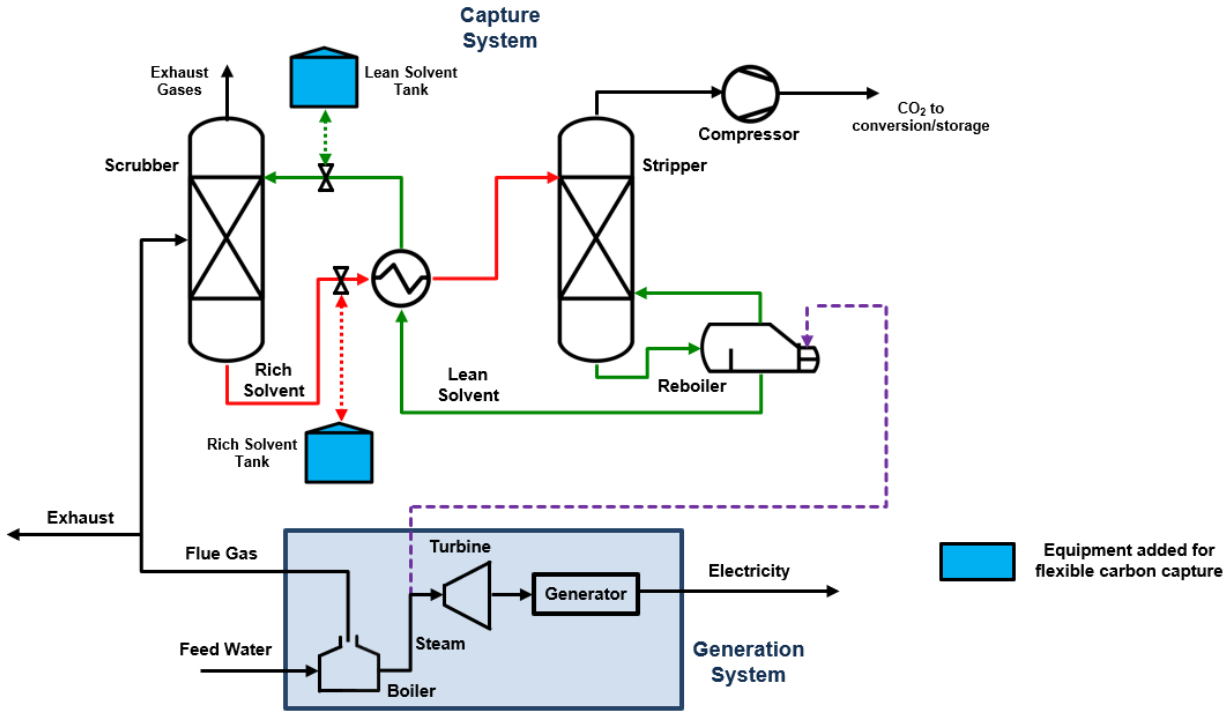

Figure 2.1: Process schematic of solvent-based post-combustion carbon capture system with solvent storage tanks for flexible operation. The rich and lean solvent storage tanks facilitate the decoupling of the power generation and CO_2 capture systems, enabling flexibility in the operation of both systems.

Developing a schedule for power generation, dispatch and utilization in power plants with flexible carbon capture systems subject to dynamically changing prices remains a relatively unexplored area. Khalilpour[49] proposed an MILP model for determining optimal multi-level carbon capture investment and operating decisions in a dynamic electricity market. They obtained a schedule for 25 years with a given electricity price profile for the first year and a constant escalation rate. Cohen

et al.[50] optimized power plant schedules under pseudo-forecasted electricity prices over one year of operation using a deterministic MILP model. They also compared the optimal profit level under varying CO_2 prices. Chen et al.[51] developed a deterministic NLP model considering day-ahead price forecasts and solvent storage. Husebye et al.[52] used an MILP model with a weekly price forecast to obtain maximum profit. However, they did not consider the effect of flexible operation on CO_2 transport and storage systems after capture. Sahraei et al.[53] developed an optimal schedule for dynamic operation by using model predictive control (MPC) under oscillatory disturbance in flue gas flowrate.

Sections 2.2 and 2.3 below elaborate more on the features of electricity and carbon markets which affect the power plant scheduling.

2.2 Electricity Market Operation Mechanism

Competitive electricity markets can be broadly categorized as either bilateral or pool-type markets, depending on how the majority of energy trading takes place. The Electric Reliability Council of Texas market (ERCOT) is an example of a bilateral market; whereas Pennsylvania, New Jersey, and Maryland (PJM) and California Independent System Operator (CAISO) are examples of pool-based markets in the US[54].

In a bilateral market, power producers and distributors enter into long-term bilateral contracts over a time period, also known as a 'contract horizon'. These contracts, facilitated by an Independent System Operator (ISO), predetermine the amount of power supplied by the generating entity to the retailer/load-serving entity along with the price over the contract horizon[55].

In contrast, a pool-type market involves short-term trading between power producers and retailers. An example of this is the 'day-ahead' scenario. A pool-based market uses a centralized auction system, where producers submit hourly power generation and selling price bids, and retailers submit power consumption and purchase price bids to a central entity: the Market Operator (MO). The MO determines the winning supply bids which meet the demand[56]. The hourly electricity supply prices determined in this way are also known as market clearing prices (MCP) or spot prices[51,55].

We assume that the energy market comprises of both pool-based and bilateral trading scenarios. The bilateral contract determines a fixed power generation schedule at a premeditated price. Power demand in excess of the contract schedule is supplied by the producer at the MCP. Moreover, we consider a day-ahead pool-based market, where electricity price forecasts are determined by the hourly supply bids for the next day. We also assume that the power producer is a price-taker in the market, i.e., hourly electricity prices are independent of net power produced by it[50]. Furthermore, subject to price volatility, we consider only the self-scheduling decisions for the producer. Bidding decisions in the day-ahead market are not considered in this work.

2.3 Carbon Market Mechanism

Typically, emission reduction is achieved by governments through either imposing a penalty on carbon emissions (carbon tax), or by setting an upper limit on carbon emissions (cap). Following the 1997 Kyoto Protocol, the European Union employed an Emissions Trading Scheme (ETS) which allow nations to put a cap on emissions using a market-based approach[57]. The ETS is a form of a cap-and-trade carbon market where a central entity (government) allocates a fixed number of emission permits, also known as carbon emission credits (CECs) across various industries. The CECs are valid for a fixed time period during which the industries can operate. During this time period, entities which exceed their quota of CECs due to higher emissions purchase CECs in the carbon market from companies with a surplus of CECs[57]. This kind of carbon trading gives an incentive to industries to reduce CO_2 emissions for maximizing their profit in the carbon market. In this work, we consider the emission regulation policy to be cap-and-trade where the government allocates 1 CEC for every metric ton of emissions. We also assume that the carbon trading takes place at the end of the day, and the carbon price throughout the day remains constant.

2.4 Research Gaps and Objectives

Based on the above review, the goal of this research is to develop a schedule of power plant operation to maximize its profit while regulating CO_2 emissions through a capture system. To this end, we outline the following research objectives:

- Compare the benefits of incorporating flexible operation in CO_2 capture systems with the conventional, fixed operation. As discussed in Section 2.1, majority of the previous works in incorporating post-combustion CO_2 capture in power plants consider steady-state operation of the capture system at some fixed, maximum load. We consider flexible operation to mitigate the high energy penalty of CO_2 capture.

- Develop a benchmark case assuming perfect foreknowledge of electricity price in the day-ahead market. We formulate a profit-maximization model of the power plant with flexible carbon capture subject to dynamically varying electricity prices. We first consider a deterministic scenario which establishes a benchmark on profit.

- Develop an optimal power production and CO_2 capture schedule under uncertainty in electricity prices. Previous literature in power plant scheduling with flexible carbon capture has primarily considered operation under a given, deterministic price profile. However, adopting the decision strategy as per the deterministic model solution can be suboptimal due to the electricity prices exhibiting high uncertainty in reality. Therefore, the deterministic model is extended to one which incorporates this uncertainty.

- Develop approximate models of optimal action policies to reduce computational complexity in the optimization framework. The hourly electricity price can assume a range of values with different probabilities associated with each value. This results in a large number of price scenarios, giving rise to the possibility of the problem 'exploding' if solved at discrete prices. To address this, the optimization problem is solved offline for a set of electricity prices to obtain approximate models of optimal action policies. These models are then used to estimate the optimal decisions for a real-time price scenario.

3. DETERMINISTIC SCHEDULING

Flexible operation of the capture system enables the power plant to strike a balance between CO_2 emissions and operational profit. To achieve an optimal trade-off, it is necessary to obtain a schedule of both the power generation and capture system operations. An optimization formulation based approach can prove to be useful in developing an optimal schedule which maximizes profit subject to various constraints. Some of the constraints which influence decision making include power generation and CO_2 capture capacity constraints, ramping constraints, solvent storage constraints and constraints on cumulative CO_2 emissions. We describe below the optimization formulation which encapsulates these different constraints to maximize the daily operational profit.

We consider a pulverized-coal fired power plant with base capacity retrofitted with the post-combustion capture system. The capture process is assumed to be absorption-based with MEA as the absorption solvent. The generation system of the power plant can adjust its power output between 300 to 600 MW. Moreover, flexible operation of the capture system is considered to be facilitated by solvent storage. We first establish a benchmark case considering a fixed price scenario. The deterministic model formulation is as follows:

Power plant decisions are assumed to have a hourly frequency. Thus, let $t \in T = \{1, 2, ..., NT\}$ represent the set of time periods in the scheduling horizon, where $NT = 24$. The variables in the deterministic model formulation are given below:

$\eta_{G,t}$: gross efficiency at hour t

$\eta^N_{G,t}$: net efficiency at hour t

$c_{G,t}$: energy generation cost per unit of total energy output at hour t in \$ MWh^{-1}

$e_{G,t}$: CO_2 emission intensity (emissions per unit of gross power output) at hour t in tons MWh^{-1}

E^N_{avg} : daily average CO_2 emission intensity

$E^N_{G,t}$: net CO_2 emission at hour t in tons

$E^S_{G,t}$: amount of compressed CO_2 exiting the capture system at hour t in tons

g_t : gross power output at hour t in MW

g^N_t : net power output at hour t in MW

L_t : solvent volume in lean solvent storage tank at hour t in m^3

$L_{t,in}$: inlet volumetric flowrate in lean solvent storage tank at hour t in m^3 hr^{-1}

$r_{A,t}$: ratio of rate of CO_2 absorbed in scrubber at hour t and CO_2 absorbed in base case operation

$r_{C,t}$: rate of CO_2 compression in compressor at hour t

$r_{D,t}$: ratio of rate of CO_2 desorbed in stripper at hour t and CO_2 desorbed in base case operation

R_t : solvent volume in rich solvent storage tank at hour t in m^3

$R_{t,in}$: inlet volumetric flowrate in rich solvent storage tank at hour t in m^3 hr^{-1}

These variables are bounded by fixed parameter values. The model also includes some key parameters. The complete list of fixed parameters along with their values assumed in the model and bounds for the variables can be found in Table 3.1.

3.1 Model Formulation

The deterministic model considered here is originally proposed by Chen et al.[51]. The objective is to maximize the total profit over one day of power plant operation with flexible carbon capture. The profit maximization model is represented as follows:

$$P0: \max \sum_{t=1}^{NT} [g^L_t \, \pi^L_G + (g^N_t - g^L_t) \, \pi^S_{G,t} - g_t \, c_{G,t}] + (E^L_G - \sum_{t=1}^{NT} E^N_{G,t}) \, \pi^L_E - \sum_{t=1}^{NT} E^S_{G,t} \, c^{TS}_S \tag{3.1a}$$

$$\text{s.t. } g^N_t = g_t - \alpha_A r_{A,t} - \alpha_D r_{D,t} \qquad \forall t \in T \tag{3.1b}$$

$$\eta_{G,t} = \omega \, (g_t - \beta)^2 + \eta_{G0} \qquad \forall t \in T \tag{3.1c}$$

$$E^N_{G,t} = \left(\frac{\eta_{G0}\, e_{G0}}{\eta_{G,t}}\right) g_t - g_0\, e_{G0}\, \gamma_A\, r_{D,t} \qquad \forall t \in T \qquad (3.1d)$$

$$E^S_{G,t} = r_{C,t}\, g_0\, e_{G0}\, \gamma_A \qquad \forall t \in T \qquad (3.1e)$$

$$r_{C,t} = r_{D,t} \qquad \forall t \in T \qquad (3.1f)$$

$$c_{G,t} = \left(\frac{\eta_{G0}\, c_{G0}}{\eta_{G,t}}\right) g_t \qquad \forall t \in T \qquad (3.1g)$$

$$g_{min} \leq g_t \leq g_0 \qquad \forall t \in T \qquad (3.1h)$$

$$0 \leq r_{A,t} \leq r_{A,max} \qquad \forall t \in T \qquad (3.1i)$$

$$0 \leq r_{D,t} \leq r_{D,max} \qquad \forall t \in T \qquad (3.1j)$$

$$-\Delta g_R \leq g_{t+1} - g_t \leq \Delta g_R \qquad \forall t \in T \setminus \{24\} \qquad (3.1k)$$

$$-\Delta r_{A,max} \leq r_{A,t+1} - r_{A,t} \leq \Delta r_{A,max} \qquad \forall t \in T \setminus \{24\} \qquad (3.1l)$$

$$-\Delta r_{D,max} \leq r_{D,t+1} - r_{D,t} \leq \Delta r_{D,max} \qquad \forall t \in T \setminus \{24\} \qquad (3.1m)$$

$$R_{t,in} = R_0\, r_{A,t} \qquad \forall t \in T \qquad (3.1n)$$

$$L_{t,in} = L_0\, r_{D,t} \qquad \forall t \in T \qquad (3.1o)$$

$$R_t = R_{0,total} + \sum_{i=1}^{t}(R_{i,in} - L_{i,in}) \qquad \forall t \in T \qquad (3.1p)$$

$$L_t = L_{0,total} + \sum_{i=1}^{t}(L_{i,in} - R_{i,in}) \qquad \forall t \in T \qquad (3.1q)$$

$$0 \leq R_t \leq R_{max} \qquad \forall t \in T \qquad (3.1r)$$

$$0 \leq L_t \leq L_{max} \qquad \forall t \in T \qquad (3.1s)$$

$$\sum_{t=1}^{NT} E^N_{G,t} - e^C_{G,max} \sum_{t=1}^{NT} g^N_t \leq 0 \qquad (3.1t)$$

The deterministic model represented by Eqs. (3.1a) - (3.1t) is a nonlinear programming (NLP) problem. Eq. (3.1a) represents the objective of profit maximization. The first term in Eq. (3.1a) is the revenue from long term bilateral contract between the distributor and power plant. The

Table 3.1: Parameter values and variable bounds.

Parameter	Significance	Unit	Value
	Key Model Parameters		
β	-	MW	550
γ_A	CO_2 removal rate of scrubber	-	85 %
η_{G0}	Base case gross efficiency	-	0.44
μ_{A0}	Base case efficiency penalty of absorption	-	0.02
μ_{B0}	Base case basic efficiency penalty	-	0.01
μ_{C0}	Base case efficiency penalty of compression	-	0.02
μ_{D0}	Base case efficiency penalty of desorption	-	0.04
π_E^L	Price of CECs in carbon market	\$ ton^{-1}	12.3
π_G^L	Average long-term contract price	\$ MWh^{-1}	51.7
ω	-	MW^{-2}	-6.4x10^{-7}
c_{G0}	Base case power generation cost	\$ MWh^{-1}	31
c_S^{TS}	Transport and storage cost of CO_2	\$ ton^{-1}	7
e_{G0}	Base case CO_2 emission intensity	tons MWh^{-1}	0.76
E_G^L	CECs allocated for one day of operation	tons	4373
$e_{G,max}^C$	Maximum CO_2 emission intensity	tons MWh^{-1}	0.3
g_0	Base case (maximum) gross power output in MW	MW	600
g_t^L	Power output as per contract schedule	MW	400
L_0	Base case inlet flowrate in lean solvent tank	m^3 hr^{-1}	7300
$L_{0,total}$	Initial solvent volume in lean solvent tank	m^3	7300
R_0	Base case inlet flowrate in rich solvent tank	m^3 hr^{-1}	7300
$R_{0,total}$	Initial solvent volume in rich solvent tank	m^3	7300
	Variable Bounds		
Δg_R	Maximum ramping rate of power generation	MW min^{-1}	6
$\Delta r_{A,max}$	Maximum ramping rate of scrubber	-	1
$\Delta r_{D,max}$	Maximum ramping rate of stripper	-	1.25
g_0	Base case (maximum) gross power output	MW	600
g_{min}	Minimum gross power output	MW	300
L_{max}	Maximum capacity of lean solvent storage tank	m^3	14600
$r_{A,max}$	Maximum CO_2 absorption rate in scrubber	-	1
$r_{D,max}$	Maximum CO_2 desorption rate in stripper	-	1.25
R_{max}	Maximum capacity of rich solvent storage tank	m^3	14600

second term is the hourly revenue generated by selling the power produced in excess of the amount determined by the contract, which is valued at the electricity spot price. The third term accounts for generation costs associated with power production. The fourth term indicates the profit obtained

from selling excess carbon credits in the cap-and-trade carbon market at the end of the day. The last term signifies transportation and storage costs associated with CO_2 capture. The key decision variables in the model are $g_t, r_{A,t}$ and $r_{D,t}$.

The details of Eqs. (3.1b)-(3.1g) can be found in Chen et al[51]. Here, only the final forms have been shown. Eq. (3.1b) computes the net power output as the reduction in gross power output due to energy consumption by absorption and desorption operations of the carbon capture system. α_A is the base case penalty due to absorption and is given by $E_0\ \mu_{A0}$, where E_0 represents the power input to the plant under base case conditions $\left(\frac{g_0}{\eta_{G0}}\right)$. Similarly, α_D represents the combined base case penalty of compression and desorption systems, and is given by $E_0\ (\mu_{D0} + \mu_{C0})$. Eq. (3.1c) represents the general relation between gross efficiency and power output for a 600 MW capacity pulverized coal based power plant. Eq. (3.1d) gives the net CO_2 emissions as the difference between the total CO_2 emissions by the generation system and CO_2 absorption in the capture system.

Eq. (3.1h) constitutes the capacity constraint of the generation system. The minimum gross power production should be a positive quantity (g_{min}) and must not exceed the production capacity of the base case plant (g_0) operating at full load conditions. Eqs. (3.1i) and (3.1j) denote capacity constraints of scrubber and stripper respectively.

Eqs. (3.1k) - (3.1m) depict ramping constraints on the generation system, scrubber and stripper, respectively. They restrict the change in gross power produced, CO_2 absorption and desorption from one time period to the next below a maximum ramping rate.

Constraints on the capacity of rich and lean solvent storage tanks are given by Eqs. (3.1n) - (3.1s). Eqs. (3.1n) - (3.1o) calculate the volumetric flowrate in rich and lean tanks as functions of the base case (fixed) inlet flowrates and amount of CO_2 processed by the capture system during flexible operation. Furthermore, Eqs. (3.1p) - (3.1q) depict volumetric flow balances to calculate solvent storage in the tanks at time t. The solvent storage in the two tanks is constrained by their maximum capacities, which are enforced by Eqs. (3.1r) - (3.1s).

Eq. (3.1t) indicates that the total CO_2 emissions in one day of operation should be below a

certain threshold value. This constraint prevents the power plant from emitting out all the CO_2 to the atmosphere to avoid expending energy in the capture system and obtaining a higher profit. This trade-off between emissions and net power output is represented through the daily average CO_2 emission intensity E^N_{avg}, where

$$E^N_{avg} = \frac{\sum_{t=1}^{NT} E^N_{G,t}}{\sum_{t=1}^{NT} g^N_t} \tag{3.2}$$

3.2 A Deterministic Case Study

Perfect foreknowledge of day-ahead electricity prices is assumed in the deterministic model. The price profile is taken from Chen et al[51]. Although they do not give the exact values, the prices are approximately taken from the price profile in their work.

The NLP model $P0$ comprises of 459 equations, 392 variables, 361 nonlinear terms and 2472 nonzero elements. It is solved to global optimality using BARON[58] v. 14.4.0 in GAMS environment. The CPU time to solve is 32 seconds on a Dell Optiplex 9020 computer (Intel 8 Core i7-4770 CPU 3.4GHz, 16.2 GB memory). The optimal total daily profit obtained is \$187,593. The different components contributing to the profit are provided in Table 3.2.

Table 3.2: Profit components in deterministic case (in \$).

Profit component	Value
Revenue from contract	496,320
Revenue in electricity spot market	107,855
Generation costs	387,595
Revenue in carbon market	16,058
Transportation and storage costs	45,044

The optimal power production schedule is given in Figure 3.1a. The price at each hour t represents the value of $\pi^S_{G,t}$ in the model. The sum of the two bars represent the gross power output

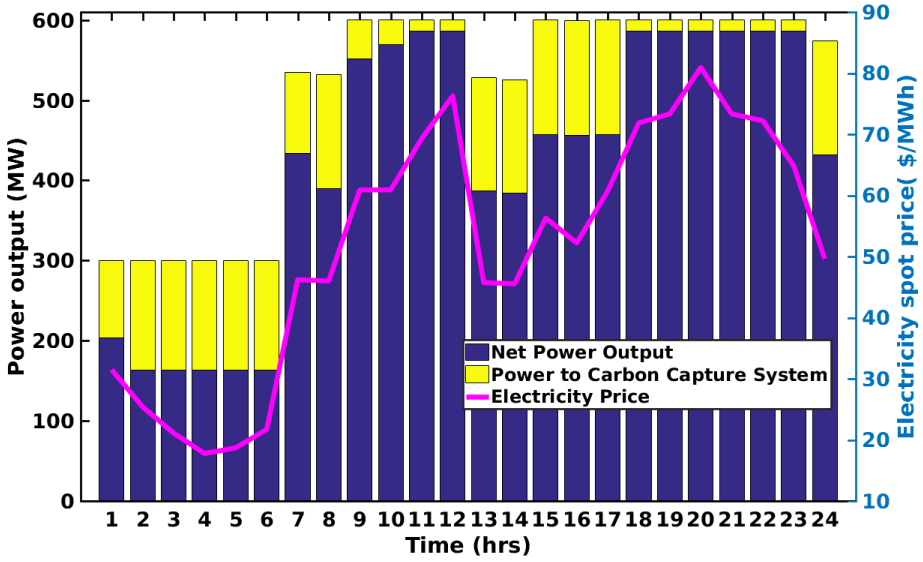

(a) Optimal power production schedule

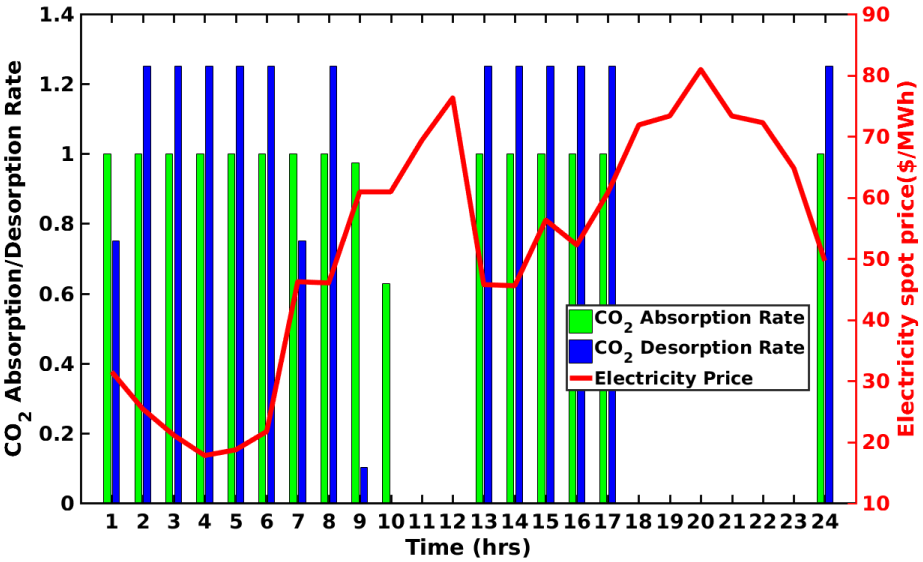

(b) Optimal CO_2 capture schedule

Figure 3.1: Optimal power plant schedule for deterministic case.

of the power plant. The result indicates that during periods of low electricity price, the gross power output is lower as compared to periods when the electricity price is high. Furthermore, more power is consumed in the capture process during low price periods than when the price is high. Thus, the

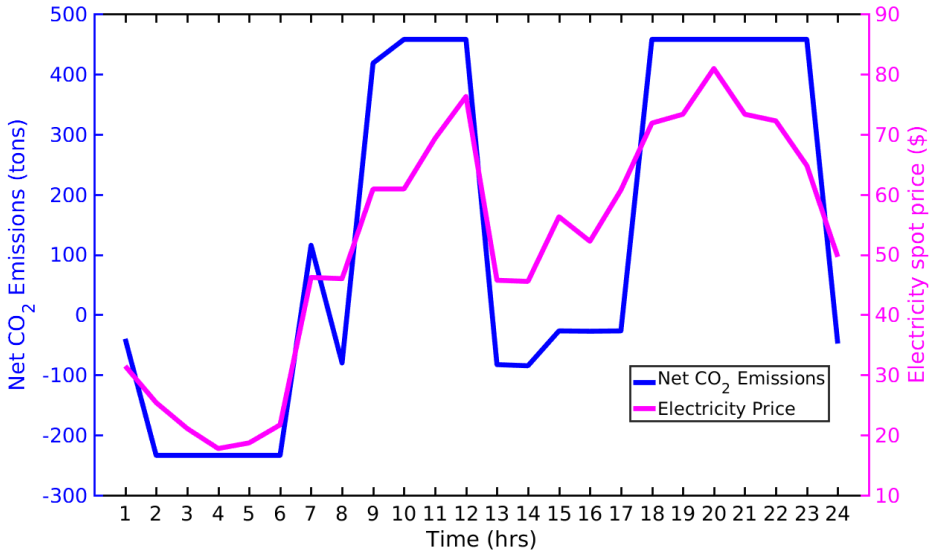

Figure 3.2: Deterministic solution: Net CO_2 emissions profile.

net power production is relatively lower when the price is low as compared to the case when the price is high.

Figure 3.1b shows the optimal CO_2 absorption and desorption rates in the scrubber and stripper respectively. It shows that during periods of low price, both CO_2 absorption and desorption are high. Additionally, in periods with high prices, both rates decrease to maximize net power output of the plant. The two rates are controlled synchronously with some exceptions over certain time intervals. The divergence is to ensure that the volume in the rich and lean solvent storage tanks does not exceed the maximum capacity.

Figure 3.2 portrays variation of net CO_2 emissions by the power plant with time. During periods of high electricity price, it is more profitable for the power plant to emit CO_2 than invest power on capturing it. This increases the net power output, resulting in higher profits. When the price drops, it is more feasible for the power plant to increase CO_2 capture. The net negative emissions during some periods of low electricity prices can be attributed to the desorption of CO_2 from the rich solvent stored when the price was relatively high. The average CO_2 emission intensity E^N_{avg} hits the the upper bound of 0.3 tons/MWh for one day. Relaxing constraint (3.1t) increases

the profit with higher CO_2 emissions. It is an environmental limitation required to keep the power plant emissions under check.

Although we have assumed that the minimum power generation is 50% of the base load (300 MW), power plants can turn down their output to as low as 20% in response to varying prices[59]. On reducing the minimum power output to 20% of the base load (120 MW), the total profit in the deterministic case increases by around 12% to $209,312. This increase in profit is due to increased revenue in the carbon trading market and reduced power generation costs.

4. MULTI-STAGE STOCHASTIC DYNAMIC OPTIMIZATION

In a competitive energy market, it is rarely that the next-day hourly electricity price profile is perfectly known[60]. Electricity price is uncertain as well as subject to dynamic changes. Addressing the uncertainty in market clearing prices is essential for power plants to develop production schedules.

To address uncertainty, several techniques are available in the literature, such as stochastic programming[61,62], robust optimization[63,64] and fuzzy programming[65,66]. Sahinidis[67] provided a detailed review of different modeling frameworks and optimization strategies under uncertainty and their application in planning and scheduling problems. Particularly in the area of scheduling for power generation, Dentcheva et al.[68] formulated a mixed-integer model with dynamic recourse for a hydro-thermal power plant under uncertainty in demand. They captured the uncertainty through a scenario tree and used a Lagrangian decomposition-based algorithm to solve the problem. Pappala et al.[69] generated scenarios to model uncertainty in load demand and intermittent wind supply and used a scenario reduction technique to make the problem computationally tractable for optimization. They then used a two-stage heuristic algorithm based on adaptive particle swarm optimization to solve the stochastic problem.

In this work, we employ a stochastic dynamic programming approach to develop an optimal operation schedule under price uncertainty. Specifically, the deterministic model described in section 3.2 is extended to a multi-stage optimization problem. We apply the recursive value iteration algorithm[70,71] to solve the problem. This algorithm, based on the Bellman equation[72], involves recursively determining an optimal 'value function'. It assumes that when a decision-maker takes a decision at a state, it receives a reward. This decision also enables reaching a future state. The value function is the optimal reward obtained at the current state. However, as per dynamic programming's 'principle of optimality', optimality is recursive in a dynamic problem and "an optimal policy has the property that whatever the initial state and initial decision are, the remaining decisions must constitute an optimal policy with regard to the state resulting from the first decision"[72].

Thus, the value function includes the maximum rewards obtained at the current state as well as the those accumulated till the end of the planning horizon. This algorithm is chosen for the current problem as we wish to determine optimal actions at each time period in the planning horizon, based on some estimate of what the price would be in the future.

To begin with, the planning horizon is divided into NT stages where $t \in T$ is the stage index. We wish to determine actions which maximize the profit obtained at each stage. The objective is obtained by considering only the time dependent terms in the objective of model $P0$ (Eq. 3.1a). Thus, the profit at each stage $t \in T$ can be expressed as

$$P_{f,t} = (g_t^N - g_t^L)\, \pi_{G,t}^S - g_t\, c_{G,t} - E_{G,t}^N\, \pi_E^L - E_{G,t}^S\, c_S^{TS} \qquad \forall t \in T \qquad (4.1)$$

Furthermore, the following sets are defined:

- **State variables**: These contain all the information required to fully determine current action to be taken and reward as a result of taking the action. At a particular time t, s_t denotes the state space vector, which includes: $\pi_{G,t}^S$ and R_t. We consider $R_t \in [0, R_{max}]$ and $\pi_{G,t}^S \in [0, \pi_{G,t}^{max}]$, where $\pi_{G,t}^{max}$ = 100. The set S_t represents all possible values that can be assumed by the state space vector s_t at time t.

- **Decision variables**: These consist of actions to be taken at the current state which results in a future state. At a particular time t, the decision variable vector is denoted by $a_t(s_t)$, which includes $g_t, r_{A,t}$ and $r_{D,t}$. The bounds on the decision variables are same as those considered in model $P0$: $g_t \in [g_{min}, g_0], r_{A,t} \in [0, r_{A,max}]$ and $r_{D,t} \in [0, r_{D,max}]$. Furthermore, A_t is the set of all possible actions that can be taken over the state space at time t.

In addition, the following attributes of the algorithm are defined:

- **Reward function**: At a particular time t, the reward function $u_t(s_t, a_t)$ consists of the immediate reward obtained from taking an action at a current state. As given by Eq. (4.1), the reward function for the stochastic counterpart is formulated by considering only the time

dependent terms in the profit expression (Eq. 3.1a) of the deterministic model. Therefore, the reward function represents immediate profit at each time step in the stochastic case. To ensure that emission intensity constraint given by Eq. (3.1t) is satisfied over the entire scheduling horizon, it is included in the reward function with a penalty parameter λ. This penalizes the profit when the constraint is violated. The immediate reward function incorporating constraint (3.1t) then becomes

$$u_t(s_t, a_t) = (g_t^N - g_t^L)\, \pi_{G,t}^S - g_t\, c_{G,t} - E_{G,t}^N\, \pi_E^L - E_{G,t}^S\, c_S^{TS} - \lambda\, (E_{G,t}^N - e_{G,max}^C\, g_t^N) \quad \forall t \in T \tag{4.2}$$

- **Transition probability function**: This denotes the probability of going from a current state $i \in S_t$ to a future state $j \in S_{t+1}$ given the decision-maker takes an action $a \in A_t$. This is represented by $P(i, a; j)$. To implement the value-iteration algorithm, it is assumed that the transition function is time-independent, resulting in a stationary stochastic process.

- **Transition equation**: This indicates the system equation establishing the relation between the current state, actions taken at the current state, and how it leads to the future state. In the deterministic model, Eq. (3.1p) calculates the total volume in the rich solvent storage tank at time t using a volumetric flow balance. As $R_0 = L_0$, Eq. (3.1p) is modified to the following form to represent the transition equation in the stochastic case

$$R_{t+1} = R_t + R_0\, (r_{A,t} - r_{D,t}) \quad \forall t \in T \tag{4.3}$$

Volumetric flow balance around the lean solvent storage tank is not considered in the transition equation as Eqs. (3.1q) and (3.1p) in model $P0$ are not independent equations.

4.1 Value Iteration Algorithm

The value iteration algorithm uses Bellman's principle of optimality[72] to recursively calculate a value function V. This recursive calculation is represented as follows using the Bellman equation:

$$V_t(s_t) = \max_{a_t \in A_t} \; u_t(s_t, a_t) + \sum_{s' \in S_{t+1}} P_t(s_t, a_t; s') \, V_{t+1}(s') \quad s_t \in S_t, \forall t \in T \tag{4.4}$$

Eq. (4.4) denotes the value function as the maximum of the sum of the current profit and expected value of the future profit. The set S_{t+1} represents all possible states at time $t+1$ and s' indicates a state space vector in this set.

Using Monte Carlo approximation[73], Eq. (4.4) can be modified to

$$V_t(s_t) \approx \max_{a_t \in A_t} \; u_t(s_t, a_t) + \frac{1}{N} \sum_{s' \in S_{t+1}} V_{t+1}(s') \quad s_t \in S_t, \forall t \in T \tag{4.5}$$

The optimal action policy at stage t constitutes the actions which provide the optimal value function. While a_t represents different possible decisions at time t, the optimal decisions are the ones which maximize the value function given by Eq. (4.5). These optimal decisions, also known as the optimal action policy, is represented as π_t as follows:

$$\pi_t(s_t) = \arg \left\{ \max_{a_t \in A_t} \; u_t(s_t, a_t) + \frac{1}{N} \sum_{s' \in S_{t+1}} V_{t+1}(s') \right\} \quad s_t \in S_t, \forall t \in T \tag{4.6}$$

In Eqs. (4.5) and (4.6), N indicates the number of possible state scenarios in the future, stage $(t+1)$, and is used to determine expected value of future profit. Therefore, there are N values of s' corresponding to each $s_t \in S_t$.

Implementing the algorithm over a discrete state space at every stage can be computationally expensive and can lead to the infamous 'curse of dimensionality' common to stochastic, dynamic optimization problems[67,74]. The challenges associated with a discrete state space can be addressed by developing approximate models for the optimal action policy and value functions at each stage

through offline optimizations. These models are then used to estimate near-optimal actions for a real-time price scenario.

The implementation of the value iteration algorithm to determine an optimal action policy under uncertainty in electricity price is described below.

4.2 Algorithm Implementation

In the multi-stage stochastic model, electricity spot price is an uncertain parameter. It can be classified as an exogenous uncertainty. This means that its possible values are independent of the action policy. To ensure that an optimal action is taken at a particular time with no prior knowledge of the future price, we adopt a two-fold approach as follows: (1) *Backward recursion*: starting at the last time period $t = NT$ and proceeding backwards, Eq. (4.6) is used recursively to get optimal action policies π_t for different state space points at each time t. This is then used to obtain approximate models of the optimal actions over the state space, (2) *Forward simulation*: the optimal action policy models determined from backward recursion are used to estimate the decisions to be taken for an electricity price scenario and calculate total optimal profit. These two processes are depicted in Figure 4.1 and are now described in detail.

4.2.1 Backward Recursion: Obtaining Optimal Action Policy

As mentioned previously, the planning horizon is divided into 24 stages and the value iteration algorithm is applied recursively on each stage to obtain the optimal action policy, $(g_t, r_{A,t}, r_{D,t})$, at different points in the state space $(\pi^S_{G,t}, R_t)$. At each time period t, the following profit maximization problem $P1$ is solved at discrete state space points s_t:

$$P1 : V_t(s_t) = \max_{a_t \in A_t(s_t)} \; u_t(s_t, a_t) + \frac{1}{N} \sum_{s' \in S_{t+1}} \widehat{V}_{t+1}(s') \tag{4.7a}$$

$$\text{s.t. } u_t = (g^N_t - g^L_t)\, \pi^S_{G,t} - g_t\, c_{G,t} - E^N_{G,t}\, \pi^L_E - E^S_{G,t}\, c^{TS}_S - \lambda\, (E^N_{G,t} - e^C_{G,max}\, g^N_t) \tag{4.7b}$$

$$g^N_t = g_t - \alpha_A r_{A,t} - \alpha_D r_{D,t} \tag{4.7c}$$

$$\eta_{G,t} = \omega\, (g_t - \beta)^2 + \eta_{G0} \tag{4.7d}$$

$$E^N_{G,t} = \left(\frac{\eta_{G0}\, e_{G0}}{\eta_{G,t}}\right) g_t - g_0\, e_{G0}\, \gamma_A\, r_{D,t} \tag{4.7e}$$

$$E^S_{G,t} = r_{C,t}\, g_0\, e_{G0}\, \gamma_A \tag{4.7f}$$

$$r_{C,t} = r_{D,t} \tag{4.7g}$$

$$c_{G,t} = \left(\frac{\eta_{G0}\, c_{G0}}{\eta_{G,t}}\right) g_t \tag{4.7h}$$

$$g_{min} \leq g_t \leq g_0 \tag{4.7i}$$

$$0 \leq r_{A,t} \leq r_{A,max} \tag{4.7j}$$

$$0 \leq r_{D,t} \leq r_{D,max} \tag{4.7k}$$

$$R_{t+1} = R_t + R_0\, (r_{A,t} - r_{D,t}) \tag{4.7l}$$

$$L_{t+1} = L_t + R_0\, (r_{D,t} - r_{A,t}) \tag{4.7m}$$

$$L_t = V_{total} - R_t \tag{4.7n}$$

$$0 \leq R_{t+1} \leq R_{max} \tag{4.7o}$$

$$0 \leq L_{t+1} \leq L_{max} \tag{4.7p}$$

$$-\Delta g_R \leq \hat{g}_{t+1}(s') - g_t \leq \Delta g_R \tag{4.7q}$$

$$-\Delta r_{A,max} \leq \hat{r}_{A,t+1}(s') - r_{A,t} \leq \Delta r_{A,max} \tag{4.7r}$$

$$-\Delta r_{D,max} \leq \hat{r}_{D,t+1}(s') - r_{D,t} \leq \Delta r_{D,max} \tag{4.7s}$$

The stochastic model $P1$ represented by Eqs. (4.7a) - (4.7s) is an NLP. The nonlinearity is due to the quadratic expression of generation efficiency given by Eq. (4.7d) and the future value function approximation $\widehat{V}_{t+1}$. The approximation process for $\widehat{V}_{t+1}$ is detailed in Section 4.2.1.2. Eqs. (4.7a) - (4.7p) are defined for $\forall t \in T$ and $s_t \in S_t$, whereas Eqs. (4.7q) - (4.7s) are defined for $\forall t \in T \setminus \{24\}$ and $s' \in S_{t+1}$.

Most of the constraints in the above stochastic model are same as in the deterministic case. The major change in the model is in the objective function given by Eq. (4.7a), with current profit

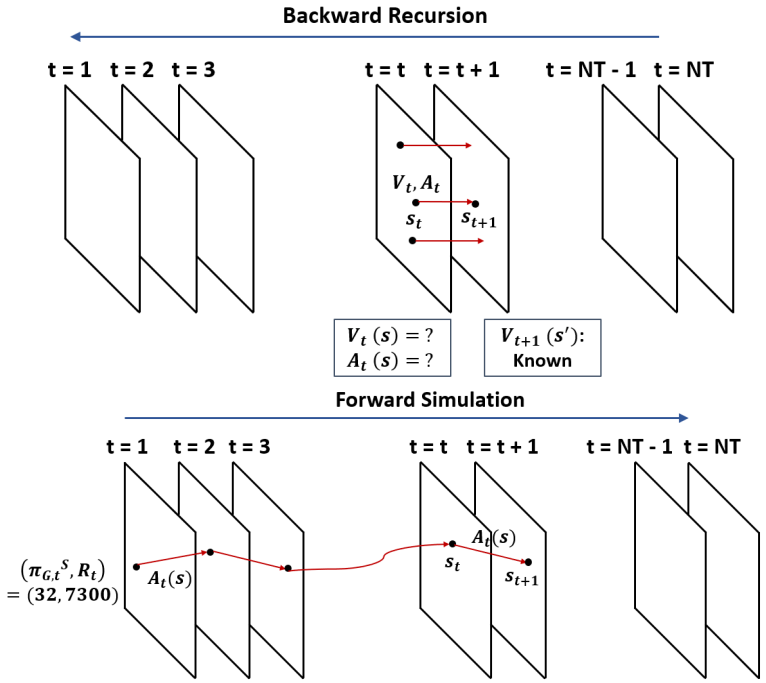

Figure 4.1: Two-fold approach in value iteration algorithm.

denoted by Eq. (4.7b). As mentioned previously, this profit includes only the time dependent terms from the objective function of the deterministic model $P0$ along with a penalty on CO_2 emissions above a threshold. Another change from the deterministic model is in the ramping constraints given by Eqs. (4.7q) - (4.7s). In these constraints, the future actions are evaluated at each of the N future state space variables. Furthermore, Eqs. (4.7l) - (4.7n) now represent the volumetric flow balance modified to give the transition equation. Eq. (4.7n) indicates that the total volume in the two tanks is constant, V_{total} = 14600, at hour t. This is derived from Eqs. (3.1p) - (3.1q) of model $P0$.

The following assumptions are made:

1. Value function at the $(NT+1)^{\text{th}}$ hour has a value of zero: $V_{NT+1} = 0$

   Typically, in value iteration, the value function corresponding to the next stage after the final one in the current planning horizon is given a fixed value. Here, it is assumed to be 0 for simplification. This transforms the objective function given by Eq. (4.7a) to:

$$V_{NT} = \max_{a_{NT} \in A_{NT}} u_{NT}(s_{NT}, a_{NT})$$

Thus, only at the last stage in the planning horizon, the optimal action policy is the one that maximizes the current profit alone, without taking into consideration the future.

2. At $t = NT + 1$, or the beginning of the next day, both storage tanks are half full of solvent, that is: $R_{NT+1} = L_{NT+1} = R_{0,total} = L_{0,total}$.

3. At each stage t, the realization of future prices (at stage $t + 1$) follows a normal distribution with current price as mean. A standard deviation of 10 is assumed, with minimum value of 0 and maximum value of 100 based on past data[75]. This can be represented as

$$\pi^S_{G,t+1} \sim N(\pi^S_{G,t}, 10^2)$$

4. $N = 100$ in Eq. (4.7a). This indicates that the objective in model $P1$ is maximizing the sum of the current profit at a particular s_t and the future profits evaluated at 100 $s' \in S_{t+1}$ points. To obtain these state space points $s' = (\pi^S_{G,t+1}, R_{t+1})$, a normal distribution is used to generate future electricity prices $\pi^S_{G,t+1}$ as per assumption 3 above. However, as shown by Eq. (4.7l), there is only one corresponding R_{t+1} for all these 100 points, obtained on solving the model.

Based on the above assumptions, model $P1$ is solved for different values of the penalty parameter λ. The significance of this parameter in the model and its effect on the algorithm implementation is discussed below.

4.2.1.1 Penalty Parameter λ

A major challenge in optimizing under uncertainty is ensuring that the cumulative CO_2 emissions are kept below the threshold value $e^C_{G,max}$. The stochastic model $P1$ lacks a cumulative constraint on CO_2 emissions similar to Eq. (3.1t) in the deterministic model. To ensure that CO_2 emissions are kept in check, the model is penalized at each time step for emissions exceeding a

certain threshold. This penalty is imposed in the offline optimization (backward recursion) process. Thus, the penalty parameter λ represents the trade-off between CO_2 emissions and power plant profit in the stochastic case. The enforcement of emission regulations and of power generating entities adhering to them is different for different locations around the world. The penalty is thereby pre-determined by the power plant operators on the basis of the amount of profit they are willing to sacrifice to keep CO_2 emissions below a certain level. We consider a representative set of 10 possible penalty parameters from $\lambda = 10$ to $\lambda = 100$ as an input to model $P1$.

Another challenge in backward recursion is the computational expense of solving model $P1$ at discrete price points at each time step. There have been many efforts in literature to reduce the computational expense associated with a discretized state space in the value-iteration algorithm. This includes approximating the value function using piecewise linear functions[76,77] and heuristic methods like neuro-dynamic programming[78]. Moreover, approximation is also required for the optimal action policies as it is be nonviable to solve the model $P1$ over the entire state space at each time t. An overview of the approach used in this work to develop approximate value function and action policy models is given below.

4.2.1.2 Approximating the Optimal Value Function and Action Policy

A precedent to deciding on the method of approximation is checking how the plot of the optimal value function: V_t and action policies: $(g_t, r_{A,t}, r_{D,t})$ looks like over the state space variables $s_t = (\pi^S_{G,t}, R_t)$. To get a representative contour plot, the state space at $t = 24$ is divided into a 20x20 grid and model $P1$ is solved for each of the 400 state space points on this grid. Figure 4.2 shows the contour of the optimal action policies and value function obtained at $t = 24$ and $t = 23$.

As can be seen from Figure 4.2, the optimal action policies and value functions are smooth over the state space at $t = 24$. Moreover, there are distinct regions in the state space where the optimal actions remain at either their upper or lower bounds. The plots also depict that the optimal action policies are more concentrated at the upper and lower bounds, with a sparse distribution in between. This is a result of the ramping constraints, Eqs. (4.7i - 4.7k) which facilitate the increase of power output through generation system from minimum to maximum load within one hour.

Moreover, the scrubber and stripper can also ramp up their load from 0 to 100% in an hour. These constraints make it possible for the power plant to operate at minimum power load and maximum capture system capacity when electricity price is low, and ramp up its operation to maximum gross power output and minimum CO_2 capture when the price is high. Thus, to maximize profit, it is be more beneficial for the power plant to set decision variables at their bounds which causes the trends seen in Figure 4.2.

However, such distinct regions are obtained only at $t = 24$ as the optimization problem involves maximizing only the current profit, without accounting for the future. For $t = 23$, the contour plots obtained do not have such distinct demarcations, as shown by Figure 4.2. This is because for all time periods except at $t = 24$, the optimal actions and value function are obtained by also accounting for N different electricity price scenarios in the future.

To globally approximate the optimal actions and value function based on solutions of $P1$ for fixed scenarios, we use ALAMO[79]. ALAMO is a data-driven, black-box modeling tool which builds compact, albeit accurate surrogate models. It uses adaptive sampling to identify deviations of the developed surrogate model from simulation. The points of model inconsistencies are added to the model training set and used to iteratively improve the model until the deviation is less than a specific tolerance[79]. ALAMO uses an external simulator to generate samples (in this case, the solution of $P1$) which gives the corresponding output variable evaluation for a given set of inputs.

The state space variables $\pi_{G,t}^{S}$ and R_t are considered as the ALAMO input variables in this work. At time t, considering the expression for $\widehat{V}_{t+1}$ is known, we wish to determine approximate models for the optimal value function V_t and decision variables $g_t, r_{A,t}, r_{D,t}$. Solving $P1$ at different state space points s_t, we pass these points and the corresponding optimal solutions as data points to ALAMO for interpolation. The output obtained from ALAMO constitutes the approximate models for V_t, $g_t, r_{A,t}$ and $r_{D,t}$. These models are passed to the previous time period as models for $\hat{V}_{t+1}(s')$, $\hat{g}_{t+1}(s')$, $\hat{r}_{A,t+1}(s')$ and $\hat{r}_{D,t+1}(s')$ in $P1$. This process is repeated till $t = 1$.

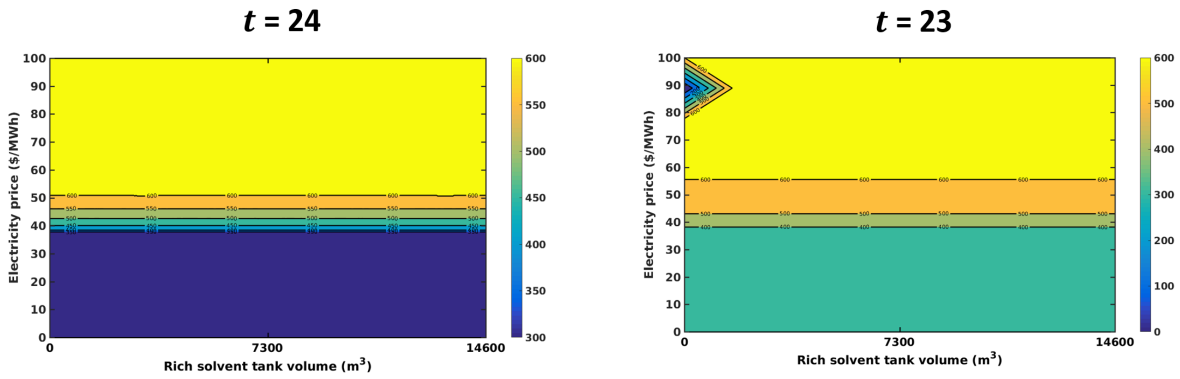

(a) Gross power generated (MW)

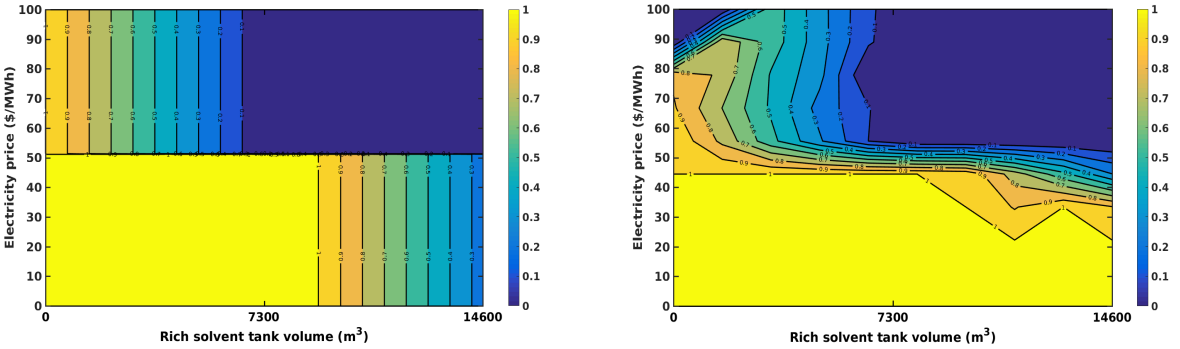

(b) Rate of CO_2 absorption

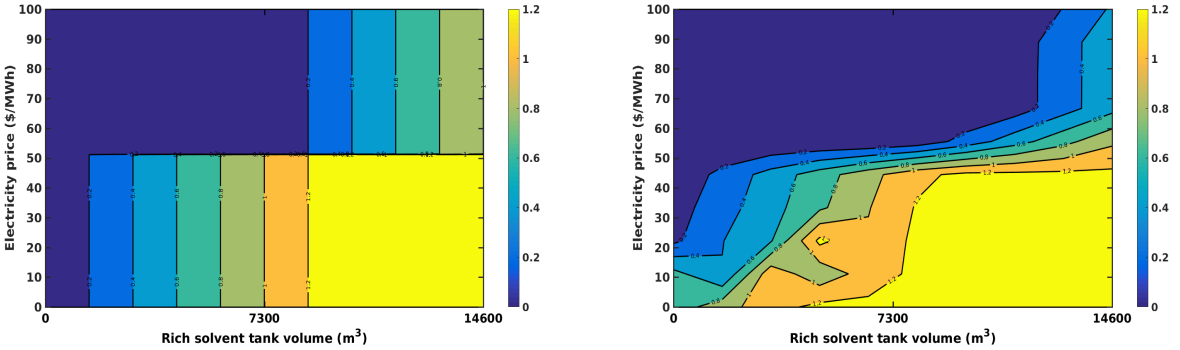

(c) Rate of CO_2 desorption

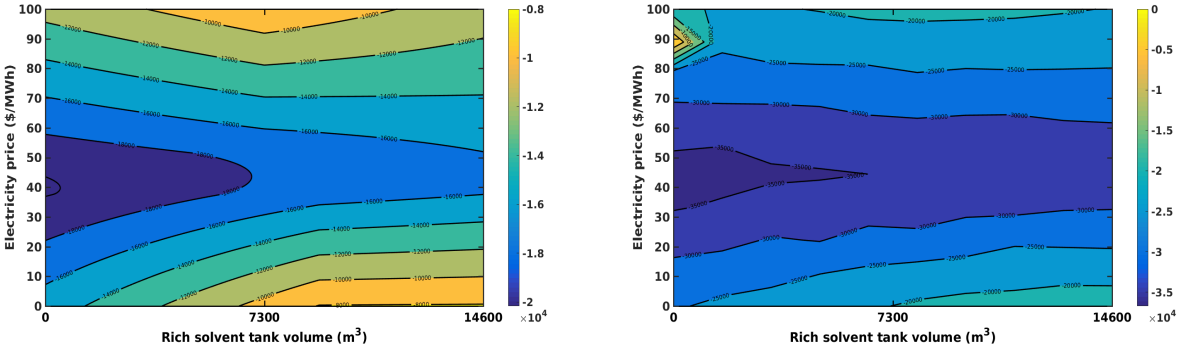

(d) Value function ($)

Figure 4.2: Contour plots of optimal value function and action policies for $t = 24$ and $t = 23$.

To avoid compromising on model accuracy as much as possible, sum of square errors (SSEp) is chosen as the fitness metric with the term penalizing the model size set to 0. At every instance of sampling, the corresponding response variables (outputs) are obtained at the sample points (inputs) by solving model $P1$ using BARON[58] solver in GAMS environment.

The complete backward recursion process is given by the flowchart in Figure 4.3.

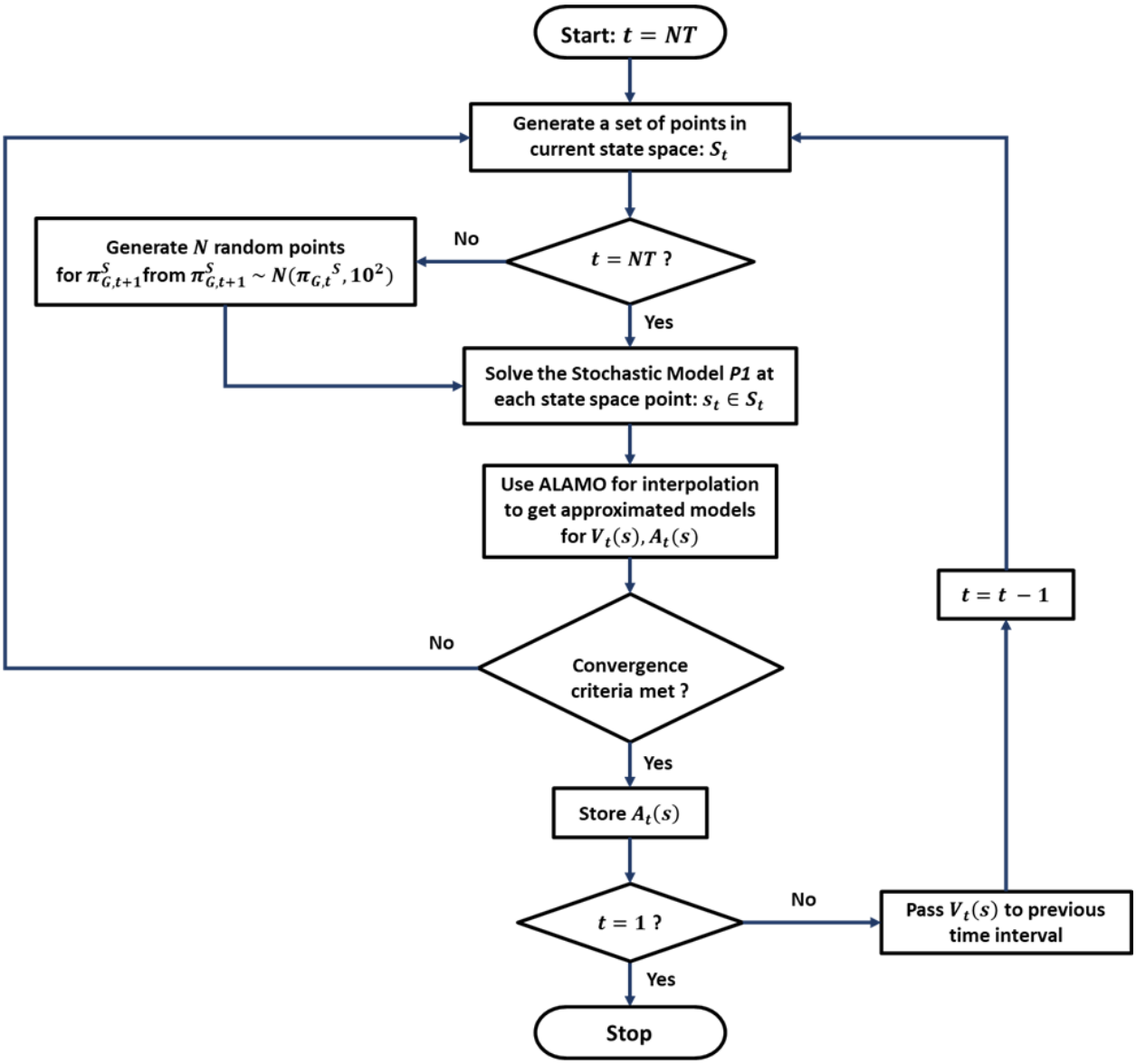

Figure 4.3: Backward recursion workflow. This process is repeated for different values of the penalty parameter λ, where λ is incremented by 10: $\lambda \in \{10,20,...,100\}$.

The match between predicted value function given by ALAMO and optimal value function is best among the four variables, with R^2 value of 0.988 for the case when penalty parameter λ = 10 and t = 24. For the same case, R^2 values of decision variables g, r_A and r_D are 0.950, 0.781 and 0.866 respectively. This indicates good fit of the generated models.

4.2.2 Forward Simulation: Calculating Total Profit

On completion of the backward recursion process, the obtained algebraic models for the optimal action policies are used to calculate the profit in the forward direction. This calculation, which does not involve any optimization is done for all stages $t \in T$.

At a particular state $s_t \in S_t$ at stage t, the optimal actions $(g_t, r_{A,t}, r_{D,t})$ are determined from the corresponding approximate models. On taking these actions, the value of the state space variable R_{t+1} at the next stage is obtained from the transition equation (Eq. 4.3). The value of the second state space variable $\pi^S_{G,t+1}$ is generated randomly from the normal distribution: $\pi^S_{G,t+1} \sim N(\pi^S_{G,t}, 10^2)$.

The reward function expression without the penalty term (Eq. 4.1) gives the profit at stage t:

$$P_{f,t} = (g^N_t - g^L_t)\, \pi^S_{G,t} - g_t\, c_{G,t} - E^N_{G,t}\, \pi^L_E - E^S_{G,t}\, c^{TS}_S \qquad \forall t \in T$$

We add together this profit from every stage along with time independent terms to get the total profit over one day of operation:

$$\text{Total profit} = \sum_{t=1}^{NT} P_{f,t} + c$$

$$\text{where, } c \text{ is constant} = \sum_{t=1}^{NT} g^L_t\, \pi^L_G + E^L_G\, \pi^L_E \tag{4.8}$$

For the starting point of the process, we assume a rich solvent volume of 7300 m^3 at the beginning of the day. Furthermore, initial electricity price of \$32 MW h^{-1} is taken, same as that in the deterministic model.

The entire forward simulation process is summarized as follows:

1. Initialize s_t = (R_t, $\pi^S_{G,t}$) to (7300, 32) at t = 1.
2. Determine the optimal action policy from the approximate models for g_t, $r_{A,t}$ and $r_{D,t}$.
3. Calculate current profit $P_{f,t}$ from Eq. (4.1).
4. To determine states at next stage, (R_{t+1}, $\pi^S_{G,t+1}$), perform the following:
   - 4.a. Calculate rich storage tank volume R_{t+1} from transition equation (Eq. 4.3).
   - 4.b. For future electricity price $\pi^S_{G,t+1}$, generate a random number from Normal distribution with mean as current price $\pi^S_{G,t}$ and standard deviation of 10.
5. If $t = NT$:

   calculate total profit. Forward simulation ends.

   Else: t = t + 1, go to step 2.

100 scenarios are generated for electricity price in the forward direction to capture uncertainty. The above process for forward simulation is repeated in its entirety for each of these 100 scenarios to calculate the optimal total profit over one day of operation. Stochasticity in electricity price is represented using a box and whisker plot, given in Figure 4.4. As the initial electricity price (at $t = 1$) is taken as \$32 MW h^{-1} for all scenarios, the price at this time is just represented by a single line instead of a range.

Forward simulation is done parallely for different values of λ to obtain optimal profit as a function of penalty parameter. This also enables determining the threshold value of λ beyond which the daily average CO_2 emissions intensity constraint (Eq. 3.1t) is met.

To summarize, the stochastic model $P1$ is solved to global optimality at different state space points $s \in S_t$ for each stage t to get interpolated functions of value function V and action policy ($g_t, r_{A,t}, r_{D,t}$). Each of the four variables have an interpolated function at every time $t \in NT$. Such interpolations at each of the ten λ values gives 4 x 24 x 10 = 960 models. The expressions for optimal action policies and value function for $\lambda = 10$ are given in the Appendix. These expressions for optimal action policy obtained as continuous functions of state space variables are then used

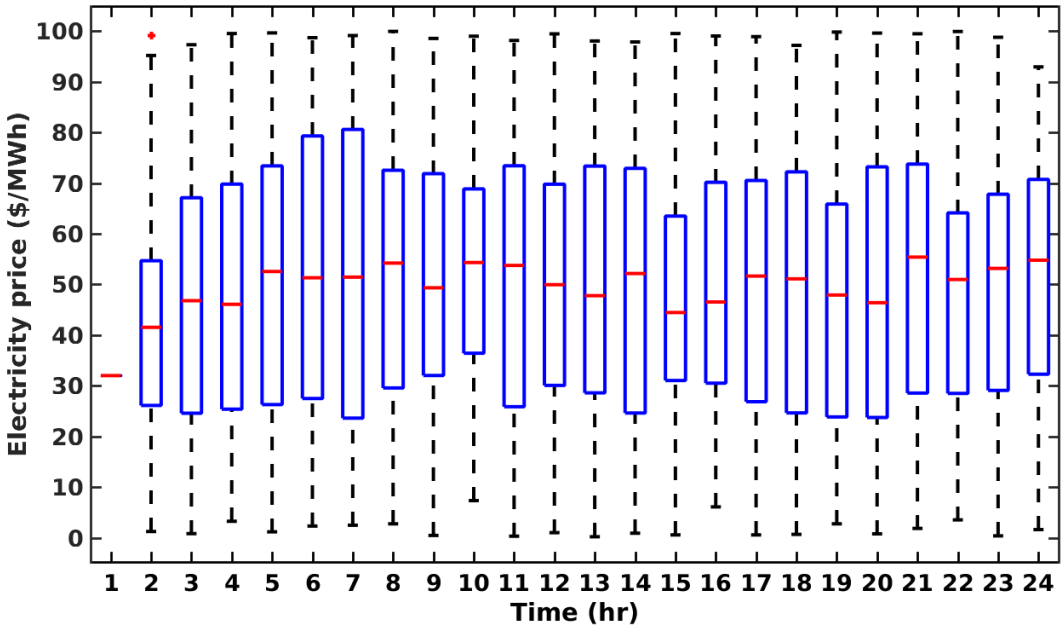

Figure 4.4: Stochasticity in electricity price. Electricity price distribution v/s time is represented through box and whisker plots. Each box at a particular time t represents distribution of price over 100 scenarios, with the red line at the middle indicating the location of midpoint (median) of the price range.

in the forward direction to determine optimal profit for different electricity price scenarios. The algorithm is implemented parallelly for different values of λ. The run time of ALAMO to approximate the optimal actions at each hour contributes to majority of the computational time in the backward recursion process. For example, the run time of ALAMO and thereby the computational time of backward recursion is approximately 18 hours for $\lambda = 10$. In contrast, forward simulation is computationally inexpensive and the time taken is negligible compared to backward recursion.

5. RESULTS AND DISCUSSION

This section elaborates on the results obtained for the price uncertainty case and comparison with the results of the deterministic model.

5.1 CO_2 Emission Intensity

The variation of daily average CO_2 emission intensity E^N_{avg} with λ is given in Figure 5.1. As λ represents the trade-off between power plant emissions and profit, for a high cost of increased emissions the power plant would take actions to lower the net CO_2 emissions. This is evident from Figure 5.1: as λ increases, E^N_{avg} follows a decreasing trend.

Figure 5.1a shows variation in the expected value of E^N_{avg} calculated over 100 scenarios for different values of λ. It depicts that the expected E^N_{avg} at λ = 10 is above the threshold emission intensity, with a large spread of data. At λ = 20, although the average E^N_{avg} lies below the threshold, the spread of the data results in some values of E^N_{avg} exceeding the threshold value. A similar trend is displayed in Figure 5.1b where the variation of E^N_{avg} with λ is shown through a box and whisker plot. From both plots, it can be safely assumed that a λ value of 30 is acceptable in satisfying the cumulative constraint on CO_2 emissions. It is difficult to determine a specific value of λ beyond which satisfying the constraint can be guaranteed, as the spread of the data changes with every new set of scenarios generated.

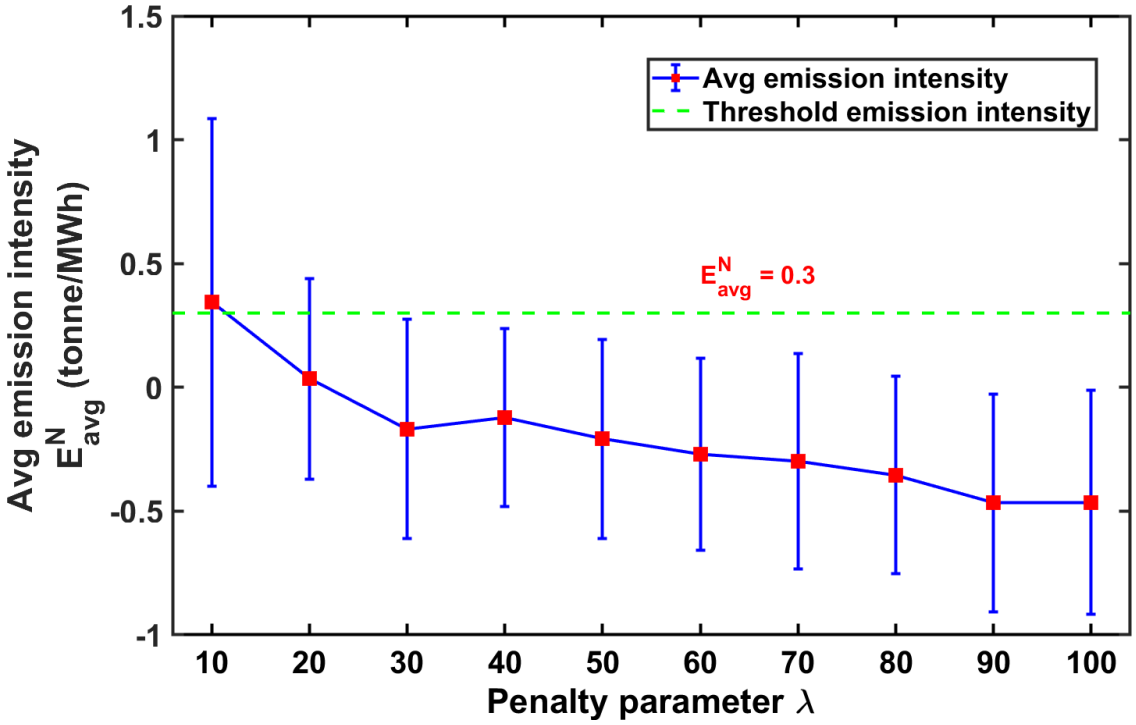

(a) Expected value and standard deviation of daily average CO_2 emission intensity at different λ.

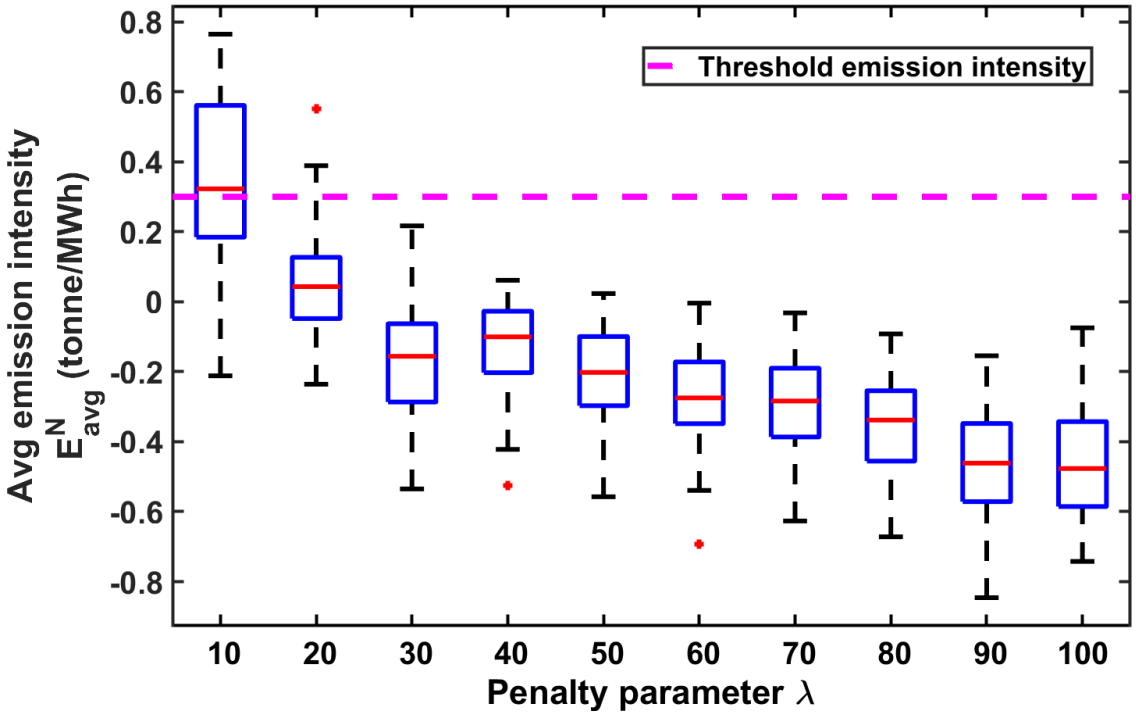

(b) Box and whisker plot of daily average CO_2 emission intensity at different λ.

Figure 5.1: Variation of daily average CO_2 emission intensity: E^N_{avg} with penalty parameter.

5.2 Total Profit

Figure 5.2 depicts variation of the total stochastic profit calculated from forward simulation for different λ values. Stochastic profit is represented as spread around an expected value, while deterministic profit is depicted only through the expected value. It is evident that as the penalty parameter λ increases, the expected value of total stochastic profit goes on decreasing. In comparison, the deterministic profit remains relatively unchanged with changing λ.

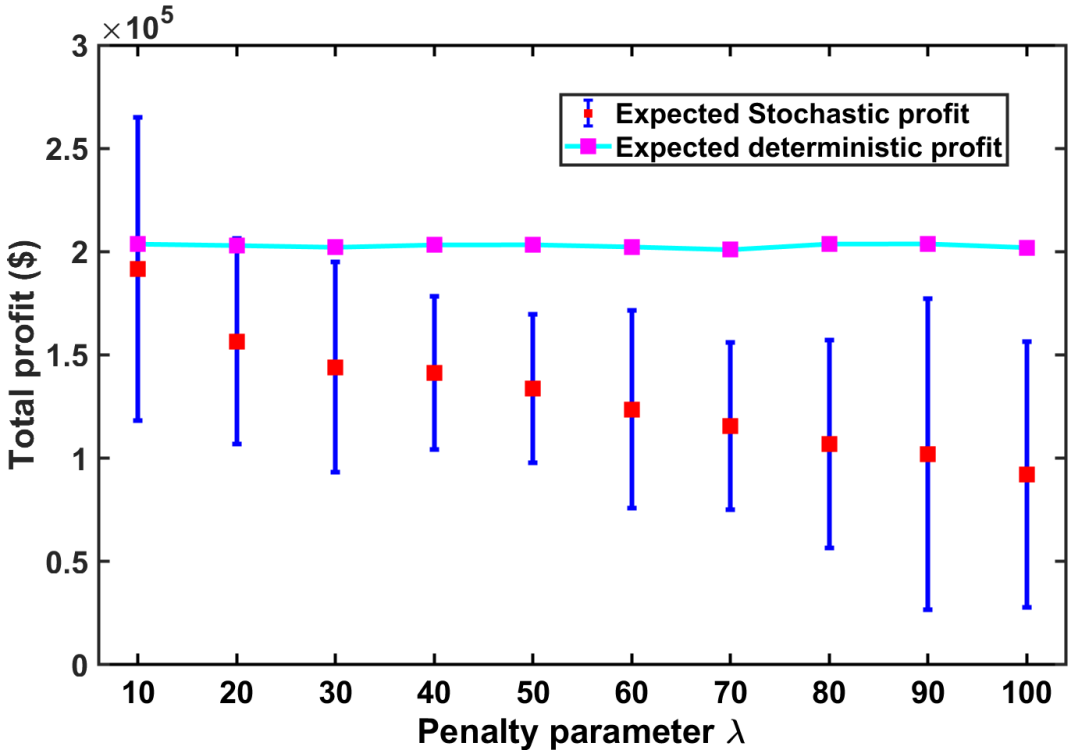

Figure 5.2: Variation of stochastic and deterministic profit with λ.

Given a price profile, the difference between the results of the two models is due to the method used to determine optimal profits. In the deterministic case, we assume perfect foreknowledge of the price profile. The deterministic profit is then obtained through optimization, by solving model $P0$. As a regulatory constraint on cumulative CO_2 emissions is included in the model through Eq. (3.1t), the optimal net power output and CO_2 emissions from this model always ensure that:

$E^N_{avg} \leq e^C_{G,max}$. Thus, the deterministic profit gives a global maxima and serves as an upper bound on profit, provided the CO_2 emissions are kept below the threshold ($e^C_{G,max}$).

On the other hand, we assume no prior knowledge of the price profile for the stochastic case. As discussed in Section 4.2.1, the optimal actions are determined through offline optimizations (backward recursion). To ensure that the cumulative CO_2 emissions are below the threshold ($e^C_{G,max}$), we penalize the objective function for emissions exceeding the threshold using a penalty parameter λ. The resulting optimal actions are approximated over the state space to get optimal action policy models at each hour. For a price scenario realization which follows the same profile as in the deterministic case, the optimal profit is then calculated using these action policy models.

This indicates that the profit obtained thereby depends on the emphasis placed on the reduction of CO_2 emissions through the penalty imposed while handling price uncertainty. When less emphasis is placed on reducing emissions by means of a low λ, the power plant emits more CO_2. This results in an increase in net power generation. Consequently, the stochastic model solution gives high profit when there is less penalty to be paid for emitting CO_2. For emissions exceeding the threshold at low penalty, the stochastic profit exceeds the deterministic profit. At sufficiently high penalty, the emissions are below the threshold and the deterministic profit gives an upper bound to the stochastic profit.

Another way of comparing deterministic and stochastic profits is through a metric called value of perfect information (VPI). VPI can be defined as the cost of uncertainty, and is given by the difference between deterministic and stochastic profits. In other words, it is the price the decision maker would pay to obtain perfect information. Variation of VPI with penalty parameter is represented through a box and whisker plot by Figure 5.3.

As the deterministic solution represents 'perfect information', VPI is typically expected to be positive. As can be seen from Figure 5.3, VPI is negative for some outliers at λ values of 10 and 20 due to the stochastic profit exceeding the deterministic one for some scenarios. As emissions decrease along with stochastic profit for increasing penalty, VPI shows an increasing trend.

As depicted by Figure 5.1, for a λ value of 30, the range of CO_2 emissions is below the thresh-

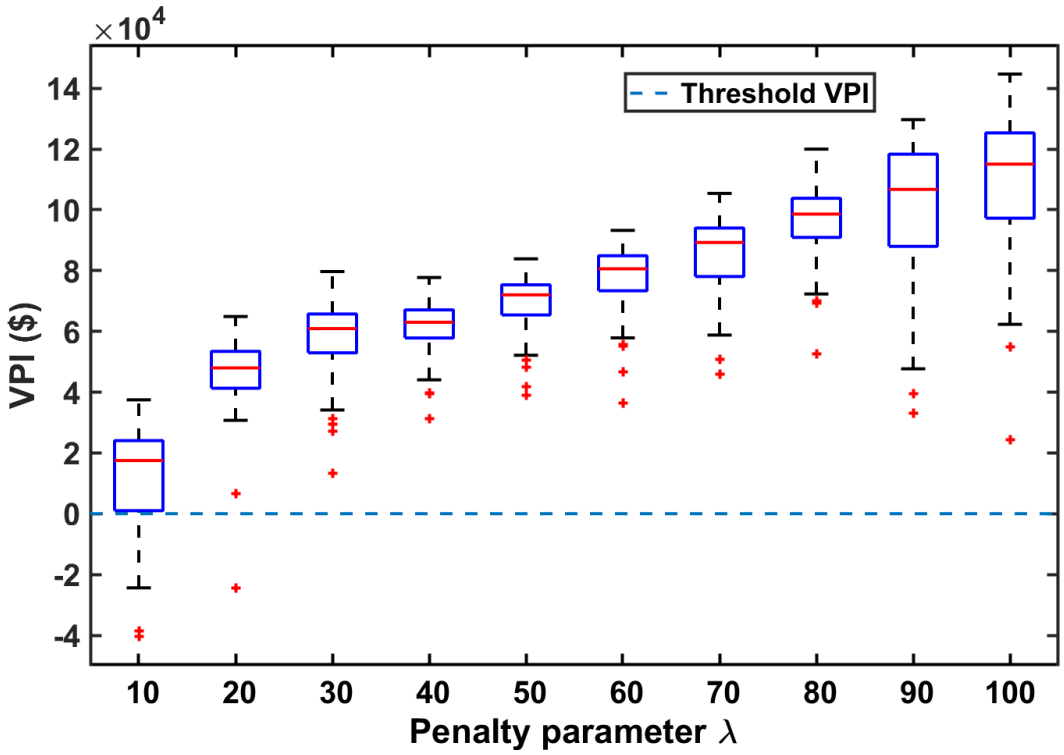

Figure 5.3: Variation of value of perfect information (VPI) with λ.

old level. At this value of the penalty parameter, the expected stochastic profit is within 25% of the expected deterministic profit, as depicted by Figure 5.2. Thus, we can say that for a satisfactory reduction of CO_2 emissions, the profit achieved under uncertainty in electricity price is within 25% of the maximum achievable profit. Moreover, to get closer to the benchmark case, other approximation methods like linear interpolation can be further applied to this problem and compared with the trade-off between accuracy and computational tractability provided by the approximate models.

5.3 Optimal Action Policy

The models for the decision variables $(g_t, r_{A,t}, r_{D,t})$ determine the hourly actions to be taken by the plant operator in face of changing electricity prices. This ensures optimal profit for any scenario realization of electricity price profile. Thus, rather than the fixed actions represented by Fig. 3.1 assuming perfect foreknowledge of electricity price, taking the actions as per the obtained

models is more beneficial to the power plant operator.

To show the effect of changing λ values on the optimal action policy, the hourly variation of decision variables for λ = 10 and λ = 100 is compared (Figure 5.4). Less emphasis is placed on emission reduction when λ = 10. As can be seen from Figure 5.4, a range of values for decision variables is obtained at each stage for λ = 10.

In comparison, the optimal action policies are different, where more emphasis is placed on emission reduction, when $\lambda = 100$. It can be seen that the optimal power generation is most concentrated at 300 MW with a few outliers. As more power generation results in higher emissions and due to the limited capacity of capture system, power generation at the minimum value of 300 MW ensures that the daily average emission intensity constraint (Eq. 3.1t) is not violated. Moreover, a similar trend is followed by CO_2 absorption rate. The rates of CO_2 absorption are mostly concentrated around the maximum value of 1, indicating more absorption to reduce CO_2 emissions. CO_2 desorption rates also show a similar pattern, with $r_{D,t}$ tending to take higher values, although there are some deviations to adjust the volume in solvent storage tanks.

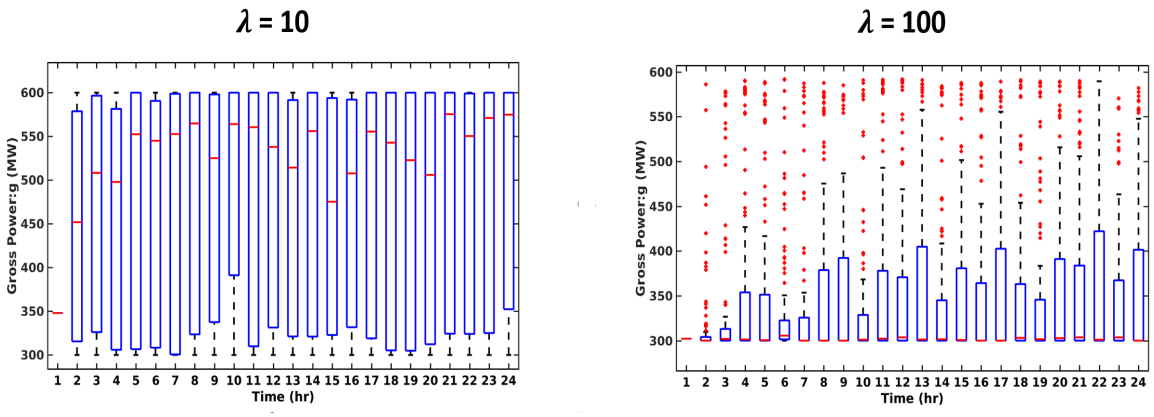

(a) Optimal gross power generation (MW)

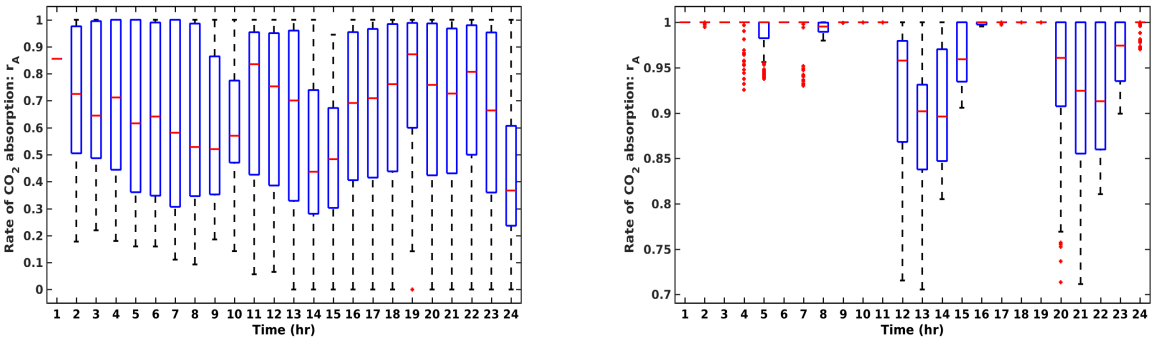

(b) Optimal rate of CO_2 absorption

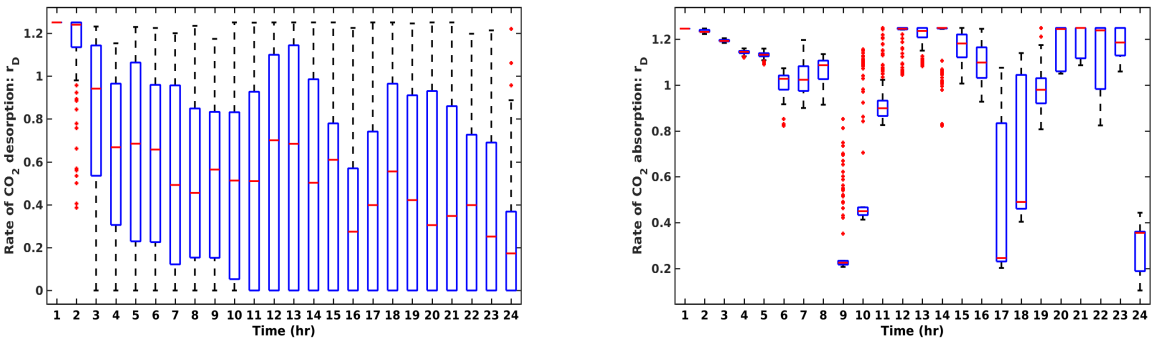

(c) Optimal rate of CO_2 desorption

Figure 5.4: Hourly optimal action policy for $\lambda = 10$ and $\lambda = 100$.

6. CONCLUSIONS AND RECOMMENDATIONS

6.1 Conclusions

Although carbon capture systems are required to reduce the high CO_2 emissions from thermal power plants, their high energy dependence restricts widespread deployment of the technology. To reduce the high energy dependence, flexible operation is considered leveraging the dynamic variation of electricity prices to vary power production as well as carbon capture operations. This work aims to develop a power production and carbon capture schedule for thermal power plants with flexibly operating carbon capture systems to achieve daily profit maximization. Compared to a conventionally considered fixed electricity price profile, uncertainty in electricity prices is incorporated to develop the schedules. A deterministic model with a fixed price profile is considered as a benchmark and is extended to include the uncertainty in electricity price along with hourly, dynamic variation. A multi-stage stochastic programming approach based on the Bellman equation is used to optimize under uncertainty in prices. To ensure that optimal actions are taken, the algorithm follows a two-fold approach: i) backward recursion and ii) forward simulation. Approximate models for optimal action policies are generated offline in the backward recursion process. These models are used to determine the actual actions and optimal profit for a real-time scenario realization of electricity price through forward simulation. This approach reduces the computational difficulties associated with optimizing repetitively for different price scenarios to get optimal schedules. Moreover, the models generated for optimal actions through backward recursion are relatively simple with fewer terms as compared to other modeling techniques like kriging and artificial neural networks, but provide higher complexity than linear interpolation. These models facilitate an optimal balance between model complexity and accuracy and are computationally advantageous due to the requirement of 24 sequential and accurate approximations.

The profit obtained when we have perfect foreknowledge of electricity price establishes a benchmark for profit under uncertainty, provided CO_2 emissions are below the threshold limit. For

the price uncertainty case, it is ensured that emissions are below the threshold through a penalty on increased emissions while determining the optimal actions offline. This penalty quantifies the trade-off between CO_2 emissions and profit. When the penalty is low, the power plant emits more CO_2, resulting in higher profits as compared to a high penalty case. Moreover, for cases when a low penalty results in emissions exceeding the threshold, the profit obtained in the uncertainty case exceeds the deterministic profit. For a high penalty, the emissions obtained when the price is uncertain are below the threshold and the deterministic model gives an upper bound on profit. Thus, the gap between the benchmark profit and the stochastic profit increases as the penalty on high emissions is increased. This gap, also indicated as the value of perfect information (VPI), denotes the price to obtain perfect knowledge of electricity price. The optimal action policy models developed in this work result in a VPI within 25% of the deterministic (maximum profit) case when CO_2 emissions from the power plant are sufficiently below the threshold value.

6.2 Recommendations for Future Work

As the surge in the use of renewables with near-zero emissions and marginal operating costs threaten to displace coal-based power generation, it is necessary for coal power plants to invest in CCS technologies that are economically viable. This research has tremendous potential in reducing the environmental footprint of coal-based power generation, making it possible for the world to continue using coal as an energy source. Although we conduct thorough research on making CCS in coal plants more cost effective through flexible operation, there is scope in further reducing the energy and cost penalty associated with CCS technologies. The following recommendations for future work have been made in this regard:

- More efficient models for the decision variables can be built through the accurate forecasting of electricity price. The number of price profiles the model is solved for in the backward recursion process can be reduced based on a probabilistic, scenario analysis.

- Renewable energy can be used to partially offset the high energy requirement of CO_2 capture. The main drawback of using renewable energy is its intermittency and unpredictable

availability. Increasing renewable penetration at the grid-level would require large-scale, capital-intensive modifications. This challenge can be addressed by using renewables to partly provide the energy requirement of CCS in coal power plants. This would prevent curtailment of excess renewable energy as well as reduce the cost of capture operation.

- An overall analysis of coal power plants with flexible carbon capture, renewables and energy storage can be considered for a decarbonized energy portfolio. Interactions between these systems can be studied at the grid level to meet electricity demand while minimizing CO_2 emissions.

REFERENCES

[1] Global energy and CO_2 status report, International Energy Agency. `http://www.iea.org/geco/`, Accessed: 16-May-2019.

[2] Solomon, S.; Plattner, G.-K.; Knutti, R.; Friedlingstein, P. Irreversible climate change due to carbon dioxide emissions. *Proceedings of the National Academy of Sciences* **2009**, *106*, 1704–1709.

[3] Hasan, M. M. F.; First, E. L.; Boukouvala, F.; Floudas, C. A. A multi-scale framework for CO_2 capture, utilization, and sequestration: CCUS and CCU. *Computers & Chemical Engineering* **2015**, *81*, 2–21.

[4] Dai, Z.; Middleton, R.; Viswanathan, H.; Fessenden-Rahn, J.; Bauman, J.; Pawar, R.; Lee, S.-Y.; McPherson, B. An integrated framework for optimizing CO_2 sequestration and enhanced oil recovery. *Environmental Science & Technology Letters* **2013**, *1*, 49–54.

[5] Aycaguer, A.-C.; Lev-On, M.; Winer, A. M. Reducing carbon dioxide emissions with enhanced oil recovery projects: A life cycle assessment approach. *Energy & Fuels* **2001**, *15*, 303–308.

[6] Hasan, M. M. F.; Boukouvala, F.; First, E. L.; Floudas, C. A. Nationwide, regional, and statewide CO_2 capture, utilization, and sequestration supply chain network optimization. *Industrial & Engineering Chemistry Research* **2014**, *53*, 7489–7506.

[7] Roh, K.; Frauzem, R.; Gani, R.; Lee, J. H. Process systems engineering issues and applications towards reducing carbon dioxide emissions through conversion technologies. *Chemical Engineering Research and Design* **2016**, *116*, 27–47.

[8] Balasubramanian, P.; Bajaj, I.; Hasan, M. M. F. Simulation and optimization of reforming reactors for carbon dioxide utilization using both rigorous and reduced models. *Journal of CO_2 Utilization* **2018**, *23*, 80–104.

[9] Iyer, S. S.; Bajaj, I.; Balasubramanian, P.; Hasan, M. M. F. Integrated carbon capture and conversion to produce syngas: novel process design, intensification, and optimization. *Industrial*

& Engineering Chemistry Research **2017**, *56*, 8622–8648.

[10] Yuan, Z.; Eden, M. R.; Gani, R. Toward the development and deployment of large-scale carbon dioxide capture and conversion processes. *Industrial & Engineering Chemistry Research* **2015**, *55*, 3383–3419.

[11] Afzal, S.; Sengupta, D.; Sarkar, A.; El-Halwagi, M.; Elbashir, N. Optimization approach to the reduction of CO_2 emissions for syngas production involving dry reforming. *ACS Sustainable Chemistry & Engineering* **2018**, *6*, 7532–7544.

[12] Global CCS Institute - Projects Database. `https://www.globalccsinstitute.com/projects/large-scale-ccs-projects`, Accessed: 14-Aug-2018.

[13] Rubin, E. S.; Chen, C.; Rao, A. B. Cost and performance of fossil fuel power plants with CO_2 capture and storage. *Energy Policy* **2007**, *35*, 4444–4454.

[14] House, K. Z.; Harvey, C. F.; Aziz, M. J.; Schrag, D. P. The energy penalty of post-combustion CO_2 capture & storage and its implications for retrofitting the US installed base. *Energy & Environmental Science* **2009**, *2*, 193–205.

[15] Mondal, M. K.; Balsora, H. K.; Varshney, P. Progress and trends in CO_2 capture/separation technologies: A review. *Energy* **2012**, *46*, 431–441.

[16] Leung, D. Y.; Caramanna, G.; Maroto-Valer, M. M. An overview of current status of carbon dioxide capture and storage technologies. *Renewable and Sustainable Energy Reviews* **2014**, *39*, 426–443.

[17] Bhown, A. S.; Freeman, B. C. Analysis and status of post-combustion carbon dioxide capture technologies. *Environmental Science & Technology* **2011**, *45*, 8624–8632.

[18] Yang, H.; Xu, Z.; Fan, M.; Gupta, R.; Slimane, R. B.; Bland, A. E.; Wright, I. Progress in carbon dioxide separation and capture: A review. *Journal of Environmental Sciences* **2008**, *20*, 14–27.

[19] Hasan, M. M. F.; Baliban, R. C.; Elia, J. A.; Floudas, C. A. Modeling, simulation, and optimization of postcombustion CO_2 capture for variable feed concentration and flow rate. 1. Chemical absorption and membrane processes. *Industrial & Engineering Chemistry Research*

2012, *51*, 15642–15664.

[20] Hasan, M. M. F.; Baliban, R. C.; Elia, J. A.; Floudas, C. A. Modeling, simulation, and optimization of postcombustion CO_2 capture for variable feed concentration and flow rate. 2. Pressure swing adsorption and vacuum swing adsorption processes. *Industrial & Engineering Chemistry Research* **2012**, *51*, 15665–15682.

[21] Hasan, M. M. F.; First, E. L.; Floudas, C. A. Cost-effective CO_2 capture based on in silico screening of zeolites and process optimization. *Physical Chemistry Chemical Physics* **2013**, *15*, 17601–17618.

[22] Aaron, D.; Tsouris, C. Separation of CO_2 from flue gas: a review. *Separation Science and Technology* **2005**, *40*, 321–348.

[23] Booth, N. Secondment to the International Test Centre for CO_2 Capture (ITC), University of Regina, Canada. January–March 2005 Report No. *COAL R303 DTI/Pub URN* **2005**, *6*, 798.

[24] Wang, M.; Lawal, A.; Stephenson, P.; Sidders, J.; Ramshaw, C. Post-combustion CO_2 capture with chemical absorption: a state-of-the-art review. *Chemical Engineering Research and Design* **2011**, *89*, 1609–1624.

[25] Davison, J. Performance and costs of power plants with capture and storage of CO_2. *Energy* **2007**, *32*, 1163–1176.

[26] Darde, V.; Van Well, W. J.; Fosboel, P. L.; Stenby, E. H.; Thomsen, K. Experimental measurement and modeling of the rate of absorption of carbon dioxide by aqueous ammonia. *International Journal of Greenhouse Gas Control* **2011**, *5*, 1149–1162.

[27] Cullinane, J. T.; Rochelle, G. T. Thermodynamics of aqueous potassium carbonate, piperazine, and carbon dioxide. *Fluid Phase Equilibria* **2005**, *227*, 197–213.

[28] Goto, K.; Yogo, K.; Higashii, T. A review of efficiency penalty in a coal-fired power plant with post-combustion CO_2 capture. *Applied Energy* **2013**, *111*, 710–720.

[29] Gibbins, J.; Crane, R.; Lambropoulos, D.; Booth, C.; Roberts, C.; Lord, M. *Greenhouse Gas Control Technologies 7*; Elsevier, 2005; pp 139–146.

[30] Gibbins, J.; Crane, R. Scope for reductions in the cost of CO_2 capture using flue gas scrubbing

with amine solvents. *Proceedings of the Institution of Mechanical Engineers, Part A: Journal of Power and Energy* **2004**, *218*, 231–239.

[31] Market Information, Electric Reliability Council of Texas (ERCOT). `www.ercot.com/mktinfo`, Accessed: 31-May-2019.

[32] Haines, M.; Davison, J. Designing carbon capture power plants to assist in meeting peak power demand. *Energy Procedia* **2009**, *1*, 1457–1464.

[33] Davidson, O.; de Coninck, H.; Loos, M.; Meyer, L. IPCC special report on carbon dioxide capture and storage. Prepared by working group III of the intergovernmental panel on climate change. 2005.

[34] Abu-Zahra, M. R.; Schneiders, L. H.; Niederer, J. P.; Feron, P. H.; Versteeg, G. F. CO_2 capture from power plants: Part I. A parametric study of the technical performance based on monoethanolamine. *International Journal of Greenhouse Gas Control* **2007**, *1*, 37–46.

[35] Abu-Zahra, M. R.; Niederer, J. P.; Feron, P. H.; Versteeg, G. F. CO_2 capture from power plants: Part II. A parametric study of the economical performance based on monoethanolamine. *International Journal of Greenhouse Gas Control* **2007**, *1*, 135–142.

[36] Artanto, Y.; Jansen, J.; Pearson, P.; Puxty, G.; Cottrell, A.; Meuleman, E.; Feron, P. Pilot-scale evaluation of AMP/PZ to capture CO_2 from flue gas of an Australian brown coal–fired power station. *International Journal of Greenhouse Gas Control* **2014**, *20*, 189–195.

[37] Lawal, A.; Wang, M.; Stephenson, P.; Koumpouras, G.; Yeung, H. Dynamic modelling and analysis of post-combustion CO_2 chemical absorption process for coal-fired power plants. *Fuel* **2010**, *89*, 2791–2801.

[38] Lucquiaud, M.; Gibbins, J. Retrofitting CO_2 capture ready fossil plants with post-combustion capture. Part 1: requirements for supercritical pulverized coal plants using solvent-based flue gas scrubbing. *Proceedings of the Institution of Mechanical Engineers, Part A: Journal of Power and Energy* **2009**, *223*, 213–226.

[39] Chalmers, H.; Lucquiaud, M.; Gibbins, J.; Leach, M. Flexible operation of coal fired power plants with postcombustion capture of carbon dioxide. *Journal of Environmental Engineering*

2009, *135*, 449–458.

[40] Mac Dowell, N.; Shah, N. Optimisation of post-combustion CO_2 capture for flexible operation. *Energy Procedia* **2014**, *63*, 1525–1535.

[41] Cohen, S. M.; Rochelle, G. T.; Webber, M. E. Optimal operation of flexible post-combustion CO_2 capture in response to volatile electricity prices. *Energy Procedia* **2011**, *4*, 2604–2611.

[42] Ziaii, S.; Cohen, S.; Rochelle, G. T.; Edgar, T. F.; Webber, M. E. Dynamic operation of amine scrubbing in response to electricity demand and pricing. *Energy Procedia* **2009**, *1*, 4047–4053.

[43] Cohen, S. M.; Rochelle, G. T.; Webber, M. E. Turning CO_2 capture on and off in response to electric grid demand: A baseline analysis of emissions and economics. *Journal of Energy Resources Technology* **2010**, *132*, 021003.

[44] Lucquiaud, M.; Fernandez, E. S.; Chalmers, H.; Mac Dowell, N.; Gibbins, J. Enhanced operating flexibility and optimised off-design operation of coal plants with post-combustion capture. *Energy Procedia* **2014**, *63*, 7494–7507.

[45] Chalmers, H.; Leach, M.; Lucquiaud, M.; Gibbins, J. Valuing flexible operation of power plants with CO_2 capture. *Energy Procedia* **2009**, *1*, 4289–4296.

[46] Chalmers, H.; Gibbins, J. Initial evaluation of the impact of post-combustion capture of carbon dioxide on supercritical pulverised coal power plant part load performance. *Fuel* **2007**, *86*, 2109–2123.

[47] Zaman, M.; Lee, J. H. Optimization of the various modes of flexible operation for post-combustion CO_2 capture plant. *Computers & Chemical Engineering* **2015**, *75*, 14–27.

[48] Patino-Echeverri, D.; Hoppock, D. C. Reducing the energy penalty costs of postcombustion CCS systems with amine-storage. *Environmental Science & Technology* **2012**, *46*, 1243–1252.

[49] Khalilpour, R. Multi-level investment planning and scheduling under electricity and carbon market dynamics: retrofit of a power plant with PCC (post-combustion carbon capture) processes. *Energy* **2014**, *64*, 172–186.

[50] Cohen, S. M.; Rochelle, G. T.; Webber, M. E. Optimizing post-combustion CO_2 capture in response to volatile electricity prices. *International Journal of Greenhouse Gas Control* **2012**, *8*, 180–195.

[51] Chen, Q.; Kang, C.; Xia, Q.; Kirschen, D. S. Optimal flexible operation of a CO_2 capture power plant in a combined energy and carbon emission market. *IEEE Transactions on Power Systems* **2012**, *27*, 1602–1609.

[52] Husebye, J.; Anantharaman, R.; Fleten, S.-E. Techno-economic assessment of flexible solvent regeneration & storage for base load coal-fired power generation with post combustion CO_2 capture. *Energy Procedia* **2011**, *4*, 2612–2619.

[53] Sahraei, M. H.; Ricardez-Sandoval, L. Controllability and optimal scheduling of a CO_2 capture plant using model predictive control. *International Journal of Greenhouse Gas Control* **2014**, *30*, 58–71.

[54] Jazayeri, P.; Schellenberg, A.; Rosehart, W.; Doudna, J.; Widergren, S.; Lawrence, D.; Mickey, J.; Jones, S. A survey of load control programs for price and system stability. *IEEE Transactions on Power Systems* **2005**, *20*, 1504–1509.

[55] Conejo, A. J.; Contreras, J.; Espinola, R.; Plazas, M. A. Forecasting electricity prices for a day-ahead pool-based electric energy market. *International Journal of Forecasting* **2005**, *21*, 435–462.

[56] Conejo, A. J.; Carrión, M.; Morales, J. M. , et al. *Decision making under uncertainty in electricity markets*; Springer, 2010; Vol. 1.

[57] Hepburn, C. Carbon trading: a review of the Kyoto mechanisms. *Annual Review of Environment and Resources* **2007**, *32*, 375–393.

[58] Sahinidis, N. V. BARON: A general purpose global optimization software package. *Journal of Global Optimization* **1996**, *8*, 201–205.

[59] Hentschel, J.; Spliethoff, H. , et al. A parametric approach for the valuation of power plant flexibility options. *Energy Reports* **2016**, *2*, 40–47.

[60] Angelus, A. Electricity price forecasting in deregulated markets. *The Electricity Journal*

2001, *14*, 32–41.

[61] Birge, J. R.; Louveaux, F. *Introduction to stochastic programming*; Springer Science & Business Media, 2011.

[62] Kall, P.; Wallace, S. W.; Kall, P. *Stochastic programming*; Springer, 1994.

[63] Ahmed, S.; Sahinidis, N. V. Robust process planning under uncertainty. *Industrial & Engineering Chemistry Research* **1998**, *37*, 1883–1892.

[64] Ben-Tal, A.; El Ghaoui, L.; Nemirovski, A. *Robust optimization*; Princeton University Press, 2009; Vol. 28.

[65] Zimmermann, H.-J. Fuzzy programming and linear programming with several objective functions. *Fuzzy Sets and Systems* **1978**, *1*, 45–55.

[66] Bellman, R. E.; Zadeh, L. A. Decision-making in a fuzzy environment. *Management Science* **1970**, *17*, B–141.

[67] Sahinidis, N. V. Optimization under uncertainty: state-of-the-art and opportunities. *Computers & Chemical Engineering* **2004**, *28*, 971–983.

[68] Dentcheva, D.; Römisch, W. *Stochastic programming methods and technical applications*; Springer, 1998; pp 22–56.

[69] Pappala, V. S.; Erlich, I.; Rohrig, K.; Dobschinski, J. A stochastic model for the optimal operation of a wind-thermal power system. *IEEE Transactions on Power Systems* **2009**, *24*, 940–950.

[70] Howard, R. A. *Dynamic programming and Markov processes*; New York: John-Wiley, 1964.

[71] Puterman, M. L. *Markov Decision Processes: Discrete Stochastic Dynamic Programming*; John Wiley & Sons, Inc., 1994.

[72] Bellman, R. E. *Dynamic Programming*; Courier Dover Publications, 1957.

[73] Gilks, W. R.; Richardson, S.; Spiegelhalter, D. *Markov chain Monte Carlo in practice*; CRC press, 1995.

[74] Si, J.; Barto, A. G.; Powell, W. B.; Wunsch, D. *Handbook of learning and approximate dynamic programming*; John Wiley & Sons, 2004; Vol. 2.

[75] Huisman, R.; Huurman, C.; Mahieu, R. Hourly electricity prices in day-ahead markets. *Energy Economics* **2007**, *29*, 240–248.

[76] Pereira, M. V.; Pinto, L. M. Multi-stage stochastic optimization applied to energy planning. *Mathematical Programming* **1991**, *52*, 359–375.

[77] De Farias, D. P.; Van Roy, B. The linear programming approach to approximate dynamic programming. *Operations Research* **2003**, *51*, 850–865.

[78] Bertsekas, D. P.; Tsitsiklis, J. N. Neuro-dynamic programming: an overview. Proceedings of the 34th IEEE Conference on Decision and Control. 1995; pp 560–564.

[79] Cozad, A.; Sahinidis, N. V.; Miller, D. C. Learning surrogate models for simulation-based optimization. *AIChE Journal* **2014**, *60*, 2211–2227.

APPENDIX A

MODELS FOR OPTIMAL DECISION VARIABLES AND VALUE FUNCTION

A.1 Input Variables

Following are the independent variables and their bounds used in model formulation:

Table A.1: Input variable set (X).

Input	System variable	Description	Lower bound	Upper bound	Unit
X_1	R_t	Volume in rich solvent storage tank	0	14,600	m^3
X_2	$\pi^S_{G,t}$	Electricity spot price	0	100	\$ MWh^{-1}

A.2 Models for Penalty parameter of 10

Table A.2: Models for gross power g_t.

Hour t	Model
1	$-0.615859\text{E} - 2X_1 - 47.715740X_2 + 0.615294X_1^{0.5} + 149.654167X_2^{0.5} + 0.156157\text{E} - 6X_1^2 + 0.979528X_2^2 - 0.249401\text{E} - 2X_2^3 - 0.114130\text{E} - 3X_2^4 + 0.782460\text{E} - 6X_2^5 + 0.421913\text{E} - 5X_1X_2 + 183.525191$
2	$-0.615828\text{E} - 2X_1 - 47.715757X_2 + 0.615266X_1^{0.5} + 149.654204X_2^{0.5} + 0.156151\text{E} - 6X_1^2 + 0.979529X_2^2 - 0.249404\text{E} - 2X_2^3 - 0.114130\text{E} - 3X_2^4 + 0.782458\text{E} - 6X_2^5 + 0.421891\text{E} - 5X_1X_2 + 183.525639$
3	$0.274375\text{E} - 2X_1 - 50.835215X_2 - 0.337286X_1^{0.5} + 157.849180X_2^{0.5} - 0.409378\text{E} - 7X_1^2 + 1.082753X_2^2 - 0.440870\text{E} - 2X_2^3 - 0.989948\text{E} - 4X_2^4 + 0.742954\text{E} - 6X_2^5 + 0.967342\text{E} - 5X_1X_2 + 205.259764$

Table A.2 – Continued

Hour t	Model
4	$-0.615823\text{E} - 2X_1 - 47.715612X_2 + 0.615262X_1^{0.5} + 149.653828X_2^{0.5} + 0.156148\text{E} - 6X_1^2 + 0.979523X_2^2 - 0.249392\text{E} - 2X_2^3 - 0.114131\text{E} - 3X_2^4 + 0.782462\text{E} - 6X_2^5 + 0.421900\text{E} - 5X_1X_2 + 183.525973$
5	$-0.615835\text{E} - 2X_1 - 47.715704X_2 + 0.615271X_1^{0.5} + 149.654059X_2^{0.5} + 0.156153\text{E} - 6X_1^2 + 0.979527X_2^2 - 0.249401\text{E} - 2X_2^3 - 0.114130\text{E} - 3X_2^4 + 0.782459\text{E} - 6X_2^5 + 0.421895\text{E} - 5X_1X_2 + 183.525640$
6	$-0.615820\text{E} - 2X_1 - 47.715487X_2 + 0.615259X_1^{0.5} + 149.653487X_2^{0.5} + 0.156147\text{E} - 6X_1^2 + 0.979519X_2^2 - 0.249384\text{E} - 2X_2^3 - 0.114132\text{E} - 3X_2^4 + 0.782465\text{E} - 6X_2^5 + 0.421907\text{E} - 5X_1X_2 + 183.526288$
7	$-0.613084\text{E} - 2X_1 - 47.699088X_2 + 0.613046X_1^{0.5} + 149.610795X_2^{0.5} + 0.155366\text{E} - 6X_1^2 + 0.978915X_2^2 - 0.248142\text{E} - 2X_2^3 - 0.114247\text{E} - 3X_2^4 + 0.782860\text{E} - 6X_2^5 + 0.421520\text{E} - 5X_1X_2 + 183.587000$
8	$-0.615796\text{E} - 2X_1 - 47.715633X_2 + 0.615241X_1^{0.5} + 149.653887X_2^{0.5} + 0.156138\text{E} - 6X_1^2 + 0.979524X_2^2 - 0.249393\text{E} - 2X_2^3 - 0.114131\text{E} - 3X_2^4 + 0.782462\text{E} - 6X_2^5 + 0.421906\text{E} - 5X_1X_2 + 183.526341$
9	$-0.615841\text{E} - 2X_1 - 47.715849X_2 + 0.615279X_1^{0.5} + 149.654408X_2^{0.5} + 0.156151\text{E} - 6X_1^2 + 0.979533X_2^2 - 0.249413\text{E} - 2X_2^3 - 0.114129\text{E} - 3X_2^4 + 0.782455\text{E} - 6X_2^5 + 0.421913\text{E} - 5X_1X_2 + 183.525414$
10	$-0.615844\text{E} - 2X_1 - 47.716021X_2 + 0.615281X_1^{0.5} + 149.654905X_2^{0.5} + 0.156156\text{E} - 6X_1^2 + 0.979538X_2^2 - 0.249424\text{E} - 2X_2^3 - 0.114128\text{E} - 3X_2^4 + 0.782451\text{E} - 6X_2^5 + 0.421889\text{E} - 5X_1X_2 + 183.524851$
11	$-0.613221\text{E} - 2X_1 - 47.699605X_2 + 0.613157X_1^{0.5} + 149.612151X_2^{0.5} + 0.155405\text{E} - 6X_1^2 + 0.978934X_2^2 - 0.248180\text{E} - 2X_2^3 - 0.114244\text{E} - 3X_2^4 + 0.782848\text{E} - 6X_2^5 + 0.421546\text{E} - 5X_1X_2 + 183.584396$

Table A.2 – Continued

Hour t	Model
12	$-0.615806\text{E} - 2X_1 - 47.715671X_2 + 0.615245X_1^{0.5} + 149.653990X_2^{0.5} + 0.156145\text{E} - 6X_1^2 + 0.979525X_2^2 - 0.249396\text{E} - 2X_2^3 - 0.114131\text{E} - 3X_2^4 + 0.782461\text{E} - 6X_2^5 + 0.421896\text{E} - 5X_1X_2 + 183.526223$
13	$-0.615818\text{E} - 2X_1 - 47.715696X_2 + 0.615258X_1^{0.5} + 149.654048X_2^{0.5} + 0.156147\text{E} - 6X_1^2 + 0.979526X_2^2 - 0.249399\text{E} - 2X_2^3 - 0.114130\text{E} - 3X_2^4 + 0.782460\text{E} - 6X_2^5 + 0.421892\text{E} - 5X_1X_2 + 183.525876$
14	$-0.615833\text{E} - 2X_1 - 47.715976X_2 + 0.615270X_1^{0.5} + 149.654776X_2^{0.5} + 0.156150\text{E} - 6X_1^2 + 0.979537X_2^2 - 0.249421\text{E} - 2X_2^3 - 0.114128\text{E} - 3X_2^4 + 0.782453\text{E} - 6X_2^5 + 0.421901\text{E} - 5X_1X_2 + 183.525326$
15	$-0.615764\text{E} - 2X_1 - 47.716435X_2 + 0.615225X_1^{0.5} + 149.655787X_2^{0.5} + 0.156123\text{E} - 6X_1^2 + 0.979559X_2^2 - 0.249475\text{E} - 2X_2^3 - 0.114122\text{E} - 3X_2^4 + 0.782430\text{E} - 6X_2^5 + 0.421879\text{E} - 5X_1X_2 + 183.525405$
16	$-0.311533\text{E} - 2X_1 - 42.859289X_2 + 0.333396X_1^{0.5} + 137.369423X_2^{0.5} + 0.105663\text{E} - 6X_1^2 + 0.789406X_2^2 + 0.163793\text{E} - 2X_2^3 - 0.155549\text{E} - 3X_2^4 + 0.936966\text{E} - 6X_2^5 + 0.536853\text{E} - 5X_1X_2 + 195.026660$
17	$-0.359174\text{E} - 2X_1 - 48.182930X_2 + 0.337740X_1^{0.5} + 150.266906X_2^{0.5} + 0.106713\text{E} - 6X_1^2 + 1.011575X_2^2 - 0.349933\text{E} - 2X_2^3 - 0.101487\text{E} - 3X_2^4 + 0.728364\text{E} - 6X_2^5 + 0.514501\text{E} - 5X_1X_2 + 190.886033$
18	$-0.693333\text{E} - 2X_1 - 47.275032X_2 + 0.661982X_1^{0.5} + 148.287852X_2^{0.5} + 0.187534\text{E} - 6X_1^2 + 0.968379X_2^2 - 0.235763\text{E} - 2X_2^3 - 0.114619\text{E} - 3X_2^4 + 0.781687\text{E} - 6X_2^5 + 0.437269\text{E} - 5X_1X_2 + 184.127138$
19	$-0.615791\text{E} - 2X_1 - 47.715594X_2 + 0.615240X_1^{0.5} + 149.653775X_2^{0.5} + 0.156134\text{E} - 6X_1^2 + 0.979522X_2^2 - 0.249391\text{E} - 2X_2^3 - 0.114131\text{E} - 3X_2^4 + 0.782463\text{E} - 6X_2^5 + 0.421918\text{E} - 5X_1X_2 + 183.526410$

Table A.2 – Continued

Hour t	Model
20	$-0.524635\text{E} - 2X_1 - 47.483018X_2 + 0.492995X_1^{0.5} + 148.687020X_2^{0.5} + 0.149211\text{E} - 6X_1^2 + 0.979268X_2^2 - 0.266731\text{E} - 2X_2^3 - 0.110890\text{E} - 3X_2^4 + 0.766118\text{E} - 6X_2^5 + 0.468284\text{E} - 5X_1X_2 + 188.136461$
21	$-0.616853\text{E} - 2X_1 - 47.721901X_2 + 0.616096X_1^{0.5} + 149.670187X_2^{0.5} + 0.156443\text{E} - 6X_1^2 + 0.979755X_2^2 - 0.249871\text{E} - 2X_2^3 - 0.114086\text{E} - 3X_2^4 + 0.782309\text{E} - 6X_2^5 + 0.422041\text{E} - 5X_1X_2 + 183.502867$
22	$-0.615824\text{E} - 2X_1 - 47.715720X_2 + 0.615265X_1^{0.5} + 149.654105X_2^{0.5} + 0.156147\text{E} - 6X_1^2 + 0.979527X_2^2 - 0.249402\text{E} - 2X_2^3 - 0.114130\text{E} - 3X_2^4 + 0.782459\text{E} - 6X_2^5 + 0.421895\text{E} - 5X_1X_2 + 183.525661$
23	$-0.571854\text{E} - 2X_1 - 48.457093X_2 + 0.601121X_1^{0.5} + 151.593133X_2^{0.5} + 0.134895\text{E} - 6X_1^2 + 1.008286X_2^2 - 0.317875\text{E} - 2X_2^3 - 0.106718\text{E} - 3X_2^4 + 0.753520\text{E} - 6X_2^5 + 0.532909\text{E} - 5X_1X_2 + 181.754533$
24	$-0.615673\text{E} - 2X_1 - 47.714105X_2 + 0.615158X_1^{0.5} + 149.650213X_2^{0.5} + 0.156101\text{E} - 6X_1^2 + 0.979461X_2^2 - 0.249255\text{E} - 2X_2^3 - 0.114144\text{E} - 3X_2^4 + 0.782511\text{E} - 6X_2^5 + 0.421793\text{E} - 5X_1X_2 + 183.528790$

Table A.3: Models for rate of CO_2 absorption $r_{A,t}$.

Hour t	Model
1	$-0.133892\text{E} - 4X_1 + 0.100752X_2 - 0.180981\text{E} - 3X_1^{0.5} - 0.283559X_2^{0.5} + 0.151676\text{E} - 9X_1^2 - 0.308166\text{E} - 2X_2^2 + 0.468019\text{E} - 4X_2^3 - 0.334544\text{E} - 6X_2^4 + 0.919186\text{E} - 9X_2^5 + 0.188915\text{E} - 7X_1X_2 + 1.278027$
2	$0.797826\text{E} - 4X_1 + 0.808634\text{E} - 1X_2 - 0.807607\text{E} - 2X_1^{0.5} - 0.239093X_2^{0.5} - 0.241166\text{E} - 8X_1^2 - 0.213254\text{E} - 2X_2^2 + 0.233127\text{E} - 4X_2^3 - 0.781870\text{E} - 7X_2^4 - 0.845222\text{E} - 10X_2^5 - 0.481187\text{E} - 7X_1X_2 + 1.399251$

Table A.3 – Continued

Hour t	Model
3	$0.318680\text{E}-4X_1+0.979775\text{E}-1X_2-0.420931\text{E}-2X_1^{0.5}-0.269243X_2^{0.5}-0.948219\text{E}-9X_1^2-0.316872\text{E}-2X_2^2+0.510785\text{E}-4X_2^3-0.388199\text{E}-6X_2^4+0.113203\text{E}-8X_2^5-0.265733\text{E}-8X_1X_2+1.342271$
4	$0.333552\text{E}-4X_1+0.660035\text{E}-1X_2-0.372824\text{E}-2X_1^{0.5}-0.192791X_2^{0.5}-0.114431\text{E}-8X_1^2-0.177946\text{E}-2X_2^2+0.193149\text{E}-4X_2^3-0.671131\text{E}-7X_2^4-0.454019\text{E}-10X_2^5-0.166519\text{E}-7X_1X_2+1.263587$
5	$0.175699\text{E}-4X_1+0.699310\text{E}-1X_2-0.197542\text{E}-2X_1^{0.5}-0.218221X_2^{0.5}-0.914592\text{E}-9X_1^2-0.151172\text{E}-2X_2^2+0.815039\text{E}-5X_2^3+0.757665\text{E}-7X_2^4-0.642998\text{E}-9X_2^5-0.198530\text{E}-7X_1X_2+1.241313$
6	$0.478160\text{E}-4X_1+0.612443\text{E}-1X_2-0.481878\text{E}-2X_1^{0.5}-0.189010X_2^{0.5}-0.171430\text{E}-8X_1^2-0.137281\text{E}-2X_2^2+0.780728\text{E}-5X_2^3+0.615899\text{E}-7X_2^4-0.546167\text{E}-9X_2^5-0.203978\text{E}-7X_1X_2+1.288127$
7	$0.436411\text{E}-4X_1+0.714481\text{E}-1X_2-0.411575\text{E}-2X_1^{0.5}-0.221337X_2^{0.5}-0.188717\text{E}-8X_1^2-0.160364\text{E}-2X_2^2+0.104894\text{E}-4X_2^3+0.493314\text{E}-7X_2^4-0.535208\text{E}-9X_2^5-0.109879\text{E}-7X_1X_2+1.294126$
8	$0.431558\text{E}-4X_1+0.491739\text{E}-1X_2-0.490182\text{E}-2X_1^{0.5}-0.149516X_2^{0.5}-0.154074\text{E}-8X_1^2-0.115592\text{E}-2X_2^2+0.511442\text{E}-5X_2^3+0.782446\text{E}-7X_2^4-0.576693\text{E}-9X_2^5+0.910791\text{E}-9X_1X_2+1.289585$
9	$0.336737\text{E}-5X_1+0.110656X_2-0.106208\text{E}-2X_1^{0.5}-0.304901X_2^{0.5}-0.562766\text{E}-9X_1^2-0.348797\text{E}-2X_2^2+0.531049\text{E}-4X_2^3-0.363871\text{E}-6X_2^4+0.915526\text{E}-9X_2^5+0.663664\text{E}-8X_1X_2+1.287038$
10	$-0.107665\text{E}-3X_1+0.117299X_2+0.648456\text{E}-2X_1^{0.5}-0.297604X_2^{0.5}+0.418015\text{E}-8X_1^2-0.448167\text{E}-2X_2^2+0.889772\text{E}-4X_2^3-0.822361\text{E}-6X_2^4+0.284432\text{E}-8X_2^5-0.114945\text{E}-6X_1X_2+1.142116$

Table A.3 – Continued

Hour t	Model
11	$0.158569\text{E}-3X_1-0.371055\text{E}-1X_2-0.145808\text{E}-1X_1^{0.5}+0.836526\text{E}-1X_2^{0.5}-0.356543\text{E}-8X_1^2+0.209140\text{E}-2X_2^2-0.591091\text{E}-4X_2^3+0.663565\text{E}-6X_2^4-0.258035\text{E}-8X_2^5-0.371096\text{E}-6X_1X_2+1.186290$
12	$0.113765\text{E}-3X_1-0.878420\text{E}-2X_2-0.104893\text{E}-1X_1^{0.5}+0.172816\text{E}-2X_2^{0.5}-0.363270\text{E}-8X_1^2+0.106284\text{E}-2X_2^2-0.401987\text{E}-4X_2^3+0.494868\text{E}-6X_2^4-0.198800\text{E}-8X_2^5-0.881809\text{E}-7X_1X_2+1.286697$
13	$0.118921\text{E}-3X_1+0.571517\text{E}-1X_2-0.104381\text{E}-1X_1^{0.5}-0.180127X_2^{0.5}-0.463122\text{E}-8X_1^2-0.127491\text{E}-2X_2^2+0.457978\text{E}-5X_2^3+0.113341\text{E}-6X_2^4-0.807179\text{E}-9X_2^5-0.865087\text{E}-8X_1X_2+1.424123$
14	$-0.105488\text{E}-3X_1-0.543884\text{E}-1X_2+0.491986\text{E}-2X_1^{0.5}+0.817441\text{E}-1X_2^{0.5}+0.623721\text{E}-9X_1^2+0.202504\text{E}-2X_2^2-0.491171\text{E}-4X_2^3+0.520841\text{E}-6X_2^4-0.197532\text{E}-8X_2^5+0.593246\text{E}-6X_1X_2+1.201116$
15	$-0.365905\text{E}-3X_1-0.499947\text{E}-1X_2+0.230343\text{E}-1X_1^{0.5}+0.128681X_2^{0.5}+0.143261\text{E}-7X_1^2+0.147567\text{E}-2X_2^2-0.271574\text{E}-4X_2^3+0.210606\text{E}-6X_2^4-0.551227\text{E}-9X_2^5+0.141223\text{E}-6X_1X_2+0.529091$
16	$0.166007\text{E}-3X_1-0.552634\text{E}-1X_2-0.140226\text{E}-1X_1^{0.5}+0.115716X_2^{0.5}-0.414260\text{E}-8X_1^2+0.297892\text{E}-2X_2^2-0.806255\text{E}-4X_2^3+0.888183\text{E}-6X_2^4-0.342241\text{E}-8X_2^5-0.202890\text{E}-6X_1X_2+1.138632$
17	$0.262602\text{E}-4X_1-0.128444X_2-0.176596\text{E}-2X_1^{0.5}+0.327972X_2^{0.5}-0.806667\text{E}-9X_1^2+0.516471\text{E}-2X_2^2-0.117839\text{E}-3X_2^3+0.117156\text{E}-5X_2^4-0.419201\text{E}-8X_2^5-0.137371\text{E}-6X_1X_2+0.817862$
18	$0.148450\text{E}-4X_1-0.114995X_2-0.121797\text{E}-2X_1^{0.5}+0.296641X_2^{0.5}-0.388087\text{E}-9X_1^2+0.461147\text{E}-2X_2^2-0.104433\text{E}-3X_2^3+0.102602\text{E}-5X_2^4-0.362701\text{E}-8X_2^5-0.164184\text{E}-6X_1X_2+0.844516$

Table A.3 – Continued

Hour t	Model
19	$0.726053\text{E}{-}4X_1{-}0.107051X_2{-}0.756423\text{E}{-}2X_1^{0.5}{+}0.271935X_2^{0.5}{-}0.163761\text{E}{-}8X_1^2+0.433161\text{E}-2X_2^2-0.981670\text{E}-4X_2^3+0.958188\text{E}-6X_2^4-0.335074\text{E}-8X_2^5-0.142905\text{E}-6X_1X_2+1.045707$
20	$0.315803\text{E}{-}4X_1{-}0.105849X_2{-}0.292494\text{E}{-}2X_1^{0.5}{+}0.275117X_2^{0.5}{-}0.872700\text{E}{-}9X_1^2+0.417589\text{E}-2X_2^2-0.927089\text{E}-4X_2^3+0.887707\text{E}-6X_2^4-0.304799\text{E}-8X_2^5-0.163793\text{E}-6X_1X_2+0.907091$
21	$0.375258\text{E}-4X_1-0.953493\text{E}-1X_2-0.313421\text{E}-2X_1^{0.5}+0.248734X_2^{0.5}-0.118288\text{E}-8X_1^2+0.377766\text{E}-2X_2^2-0.836521\text{E}-4X_2^3+0.794344\text{E}-6X_2^4-0.270114\text{E}-8X_2^5-0.195731\text{E}-6X_1X_2+0.917441$
22	$0.648702\text{E}{-}4X_1{-}0.103298X_2{-}0.696106\text{E}{-}2X_1^{0.5}{+}0.267650X_2^{0.5}{-}0.133476\text{E}{-}8X_1^2+0.414933\text{E}-2X_2^2-0.924453\text{E}-4X_2^3+0.885846\text{E}-6X_2^4-0.304218\text{E}-8X_2^5-0.282234\text{E}-6X_1X_2+1.033070$
23	$0.148612\text{E}{-}3X_1{-}0.107786X_2{-}0.152988\text{E}{-}1X_1^{0.5}{+}0.287179X_2^{0.5}{-}0.314149\text{E}{-}8X_1^2+0.432647\text{E}-2X_2^2-0.962110\text{E}-4X_2^3+0.923110\text{E}-6X_2^4-0.316868\text{E}-8X_2^5-0.563909\text{E}-6X_1X_2+1.216738$
24	$0.238511\text{E}{-}3X_1{-}0.219043X_2{-}0.250696\text{E}{-}1X_1^{0.5}{+}0.566625X_2^{0.5}{-}0.750237\text{E}{-}8X_1^2+0.894924\text{E}-2X_2^2-0.209734\text{E}-3X_2^3+0.217482\text{E}-5X_2^4-0.811099\text{E}-8X_2^5-0.469981\text{E}-6X_1X_2+1.369160$

Table A.4: Models for rate of CO_2 desorption $r_{D,t}$.

Hour t	Model
1	$-0.363146\text{E}-4X_1-0.377439\text{E}-2X_2+0.734809\text{E}-2X_1^{0.5}+0.226600\text{E}-2X_2^{0.5}-0.634753\text{E}-9X_1^2-0.858979\text{E}-4X_2^2+0.648535\text{E}-5X_2^3-0.147347\text{E}-6X_2^4+0.830200\text{E}-9X_2^5+0.474815\text{E}-6X_1X_2+0.949011$

Table A.4 – Continued

Hour t	Model
2	$-0.139230\text{E} - 3X_1 - 0.278775\text{E} - 1X_2 + 0.176639\text{E} - 1X_1^{0.5} + 0.808304\text{E} - 1X_2^{0.5} + 0.203365\text{E} - 8X_1^2 + 0.697608\text{E} - 3X_2^2 - 0.836305\text{E} - 5X_2^3 - 0.145181\text{E} - 7X_2^4 + 0.386647\text{E} - 9X_2^5 + 0.271475\text{E} - 6X_1X_2 + 0.619123$
3	$-0.134095\text{E} - 3X_1 + 0.111551\text{E} - 1X_2 + 0.166476\text{E} - 1X_1^{0.5} - 0.268771\text{E} - 1X_2^{0.5} + 0.201280\text{E} - 8X_1^2 - 0.735176\text{E} - 3X_2^2 + 0.229310\text{E} - 4X_2^3 - 0.329302\text{E} - 6X_2^4 + 0.154191\text{E} - 8X_2^5 + 0.338391\text{E} - 6X_1X_2 + 0.733077$
4	$-0.137439\text{E} - 3X_1 - 0.416174\text{E} - 1X_2 + 0.169024\text{E} - 1X_1^{0.5} + 0.121381X_2^{0.5} + 0.233852\text{E} - 8X_1^2 + 0.113579\text{E} - 2X_2^2 - 0.157443\text{E} - 4X_2^3 + 0.364195\text{E} - 7X_2^4 + 0.278284\text{E} - 9X_2^5 + 0.195737\text{E} - 6X_1X_2 + 0.622256$
5	$-0.145512\text{E} - 3X_1 - 0.855213\text{E} - 1X_2 + 0.165289\text{E} - 1X_1^{0.5} + 0.239179X_2^{0.5} + 0.302956\text{E} - 8X_1^2 + 0.272065\text{E} - 2X_2^2 - 0.486476\text{E} - 4X_2^3 + 0.343562\text{E} - 6X_2^4 - 0.756131\text{E} - 9X_2^5 + 0.157690\text{E} - 6X_1X_2 + 0.593491$
6	$-0.135207\text{E} - 3X_1 - 0.104774X_2 + 0.152276\text{E} - 1X_1^{0.5} + 0.287016X_2^{0.5} + 0.287891\text{E} - 8X_1^2 + 0.349471\text{E} - 2X_2^2 - 0.668337\text{E} - 4X_2^3 + 0.536065\text{E} - 6X_2^4 - 0.149090\text{E} - 8X_2^5 + 0.176535\text{E} - 6X_1X_2 + 0.607941$
7	$-0.118031\text{E} - 3X_1 - 0.820327\text{E} - 1X_2 + 0.138739\text{E} - 1X_1^{0.5} + 0.226309X_2^{0.5} + 0.220904\text{E} - 8X_1^2 + 0.259177\text{E} - 2X_2^2 - 0.459161\text{E} - 4X_2^3 + 0.314387\text{E} - 6X_2^4 - 0.637013\text{E} - 9X_2^5 + 0.242403\text{E} - 6X_1X_2 + 0.675538$
8	$-0.115421\text{E} - 3X_1 - 0.887871\text{E} - 1X_2 + 0.134781\text{E} - 1X_1^{0.5} + 0.237244X_2^{0.5} + 0.212649\text{E} - 8X_1^2 + 0.296032\text{E} - 2X_2^2 - 0.570290\text{E} - 4X_2^3 + 0.453424\text{E} - 6X_2^4 - 0.123011\text{E} - 8X_2^5 + 0.331970\text{E} - 6X_1X_2 + 0.690514$
9	$-0.110723\text{E} - 3X_1 - 0.111606\text{E} - 2X_2 + 0.144356\text{E} - 1X_1^{0.5} - 0.216090\text{E} - 2X_2^{0.5} + 0.137083\text{E} - 8X_1^2 - 0.133470\text{E} - 3X_2^2 + 0.600641\text{E} - 5X_2^3 - 0.125670\text{E} - 6X_2^4 + 0.694589\text{E} - 9X_2^5 + 0.423319\text{E} - 6X_1X_2 + 0.775922$

Table A.4 – Continued

Hour t	Model
10	$-0.142969\text{E} - 3X_1 + 0.813781\text{E} - 2X_2 + 0.201822\text{E} - 1X_1^{0.5} + 0.272660\text{E} - 2X_2^{0.5} + 0.151966\text{E} - 8X_1^2 - 0.777239\text{E} - 3X_2^2 + 0.277037\text{E} - 4X_2^3 - 0.402380\text{E} - 6X_2^4 + 0.186562\text{E} - 8X_2^5 - 0.474554\text{E} - 7X_1X_2 + 0.516190$
11	$-0.295382\text{E} - 3X_1 - 0.121877X_2 + 0.301776\text{E} - 1X_1^{0.5} + 0.346713X_2^{0.5} + 0.783285\text{E} - 8X_1^2 + 0.424770\text{E} - 2X_2^2 - 0.847578\text{E} - 4X_2^3 + 0.741423\text{E} - 6X_2^4 - 0.236240\text{E} - 8X_2^5 - 0.318203\text{E} - 6X_1X_2 + 0.173826$
12	$0.618331\text{E} - 5X_1 - 0.157778X_2 - 0.111164\text{E} - 2X_1^{0.5} + 0.402991X_2^{0.5} + 0.635634\text{E} - 9X_1^2 + 0.607585\text{E} - 2X_2^2 - 0.134676\text{E} - 3X_2^3 + 0.130545\text{E} - 5X_2^4 - 0.456753\text{E} - 8X_2^5 + 0.861544\text{E} - 7X_1X_2 + 1.013913$
13	$0.382219\text{E} - 4X_1 - 0.134936X_2 - 0.347068\text{E} - 2X_1^{0.5} + 0.329238X_2^{0.5} - 0.889985\text{E} - 9X_1^2 + 0.527162\text{E} - 2X_2^2 - 0.119426\text{E} - 3X_2^3 + 0.117085\text{E} - 5X_2^4 - 0.411865\text{E} - 8X_2^5 + 0.440841\text{E} - 6X_1X_2 + 1.125117$
14	$0.621613\text{E} - 4X_1 - 0.394891\text{E} - 1X_2 - 0.230367\text{E} - 2X_1^{0.5} + 0.632390\text{E} - 1X_2^{0.5} - 0.321312\text{E} - 8X_1^2 + 0.165032\text{E} - 2X_2^2 - 0.421015\text{E} - 4X_2^3 + 0.441347\text{E} - 6X_2^4 - 0.165267\text{E} - 8X_2^5 + 0.856002\text{E} - 6X_1X_2 + 1.165153$
15	$0.162951\text{E} - 3X_1 - 0.828274\text{E} - 1X_2 + 0.463072\text{E} - 4X_1^{0.5} + 0.199317X_2^{0.5} - 0.114439\text{E} - 7X_1^2 + 0.334602\text{E} - 2X_2^2 - 0.793689\text{E} - 4X_2^3 + 0.833470\text{E} - 6X_2^4 - 0.318879\text{E} - 8X_2^5 + 0.109982\text{E} - 6X_1X_2 + 0.712765$
16	$-0.370841\text{E} - 3X_1 - 0.128881X_2 + 0.366395\text{E} - 1X_1^{0.5} + 0.344830X_2^{0.5} + 0.101086\text{E} - 7X_1^2 + 0.533196\text{E} - 2X_2^2 - 0.127276\text{E} - 3X_2^3 + 0.132834\text{E} - 5X_2^4 - 0.500039\text{E} - 8X_2^5 - 0.421958\text{E} - 6X_1X_2 + 0.497607\text{E} - 1$
17	$0.200640\text{E} - 4X_1 + 0.602515\text{E} - 3X_2 - 0.326606\text{E} - 2X_1^{0.5} - 0.689618\text{E} - 2X_2^{0.5} + 0.107808\text{E} - 8X_1^2 + 0.333770\text{E} - 3X_2^2 - 0.195831\text{E} - 4X_2^3 + 0.258313\text{E} - 6X_2^4 - 0.104741\text{E} - 8X_2^5 - 0.133608\text{E} - 6X_1X_2 + 1.303197$

Table A.4 – Continued

Hour t	Model
18	$0.931939\text{E}-4X_1+0.595380\text{E}-1X_2-0.981633\text{E}-2X_1^{0.5}-0.152879X_2^{0.5}-0.696368\text{E}-9X_1^2-0.204890\text{E}-2X_2^2+0.345942\text{E}-4X_2^3-0.289174\text{E}-6X_2^4+0.942493\text{E}-9X_2^5-0.205706\text{E}-6X_1X_2+1.512320$
19	$0.341740\text{E}-4X_1-0.631958\text{E}-1X_2-0.125598\text{E}-2X_1^{0.5}+0.189541X_2^{0.5}-0.271449\text{E}-9X_1^2+0.198501\text{E}-2X_2^2-0.441949\text{E}-4X_2^3+0.420825\text{E}-6X_2^4-0.141401\text{E}-8X_2^5-0.126908\text{E}-6X_1X_2+0.996647$
20	$0.121209\text{E}-3X_1-0.593755\text{E}-1X_2-0.129436\text{E}-1X_1^{0.5}+0.147834X_2^{0.5}-0.145540\text{E}-8X_1^2+0.251776\text{E}-2X_2^2-0.676048\text{E}-4X_2^3+0.741635\text{E}-6X_2^4-0.282128\text{E}-8X_2^5-0.220433\text{E}-7X_1X_2+1.440634$
21	$0.218982\text{E}-3X_1+0.236188\text{E}-1X_2-0.214138\text{E}-1X_1^{0.5}-0.493859\text{E}-1X_2^{0.5}-0.380922\text{E}-8X_1^2-0.108642\text{E}-2X_2^2+0.176802\text{E}-4X_2^3-0.148722\text{E}-6X_2^4+0.520890\text{E}-9X_2^5-0.873030\text{E}-7X_1X_2+1.692309$
22	$0.506518\text{E}-4X_1-0.146674X_2+0.430501\text{E}-3X_1^{0.5}+0.396702X_2^{0.5}-0.433541\text{E}-9X_1^2+0.527962\text{E}-2X_2^2-0.120705\text{E}-3X_2^3+0.124527\text{E}-5X_2^4-0.465217\text{E}-8X_2^5-0.282869\text{E}-6X_1X_2+0.624189$
23	$0.393103\text{E}-3X_1-0.639995\text{E}-1X_2-0.390806\text{E}-1X_1^{0.5}+0.164418X_2^{0.5}-0.777199\text{E}-8X_1^2+0.213808\text{E}-2X_2^2-0.532974\text{E}-4X_2^3+0.575623\text{E}-6X_2^4-0.219910\text{E}-8X_2^5+0.161588\text{E}-6X_1X_2+2.022054$
24	$0.375497\text{E}-3X_1-0.219043X_2-0.250696\text{E}-1X_1^{0.5}+0.566625X_2^{0.5}-0.750237\text{E}-8X_1^2+0.894924\text{E}-2X_2^2-0.209734\text{E}-3X_2^3+0.217482\text{E}-5X_2^4-0.811099\text{E}-8X_2^5-0.469981\text{E}-6X_1X_2+0.369160$

Table A.5: Models for value function V_t.

Hour t	Model
1	$0.649878X_1 + 2296.628784X_2 - 12.723415X_1^{0.5} - 6539.962585X_2^{0.5} - 0.141041\text{E} - 4X_1^2 - 141.330757X_2^2 + 3.029752X_2^3 - 0.250226\text{E} - 1X_2^4 + 0.717401\text{E} - 4X_2^5 - 0.590248\text{E} - 2X_1X_2 - 312649.681050$
2	$0.223343X_1 + 2145.344224X_2 + 9.684335X_1^{0.5} - 6070.647489X_2^{0.5} + 0.151655\text{E} - 5X_1^2 - 136.780729X_2^2 + 2.947198X_2^3 - 0.243496\text{E} - 1X_2^4 + 0.697870\text{E} - 4X_2^5 - 0.552429\text{E} - 2X_1X_2 - 298898.600510$
3	$0.867813X_1 + 2146.804259X_2 - 44.797266X_1^{0.5} - 6097.530708X_2^{0.5} - 0.153054\text{E} - 4X_1^2 - 136.863953X_2^2 + 2.953843X_2^3 - 0.244579\text{E} - 1X_2^4 + 0.703624\text{E} - 4X_2^5 - 0.587200\text{E} - 2X_1X_2 - 284061.446995$
4	$0.561508X_1 + 2217.304223X_2 - 17.143861X_1^{0.5} - 6273.709487X_2^{0.5} - 0.661349\text{E} - 5X_1^2 - 139.018660X_2^2 + 2.988392X_2^3 - 0.246603\text{E} - 1X_2^4 + 0.705494\text{E} - 4X_2^5 - 0.596577\text{E} - 2X_1X_2 - 270685.992810$
5	$0.734027X_1 + 2257.292158X_2 - 30.496921X_1^{0.5} - 6390.147734X_2^{0.5} - 0.113842\text{E} - 4X_1^2 - 140.228267X_2^2 + 3.012368X_2^3 - 0.248885\text{E} - 1X_2^4 + 0.713635\text{E} - 4X_2^5 - 0.590330\text{E} - 2X_1X_2 - 256547.798833$
6	$0.727425X_1 + 2250.086087X_2 - 27.694629X_1^{0.5} - 6373.125420X_2^{0.5} - 0.117774\text{E} - 4X_1^2 - 139.862927X_2^2 + 3.006376X_2^3 - 0.248501\text{E} - 1X_2^4 + 0.712721\text{E} - 4X_2^5 - 0.578353\text{E} - 2X_1X_2 - 242803.102431$
7	$0.762673X_1 + 2264.706488X_2 - 28.156741X_1^{0.5} - 6425.988361X_2^{0.5} - 0.141526\text{E} - 4X_1^2 - 140.212224X_2^2 + 3.018063X_2^3 - 0.250107\text{E} - 1X_2^4 + 0.719600\text{E} - 4X_2^5 - 0.570159\text{E} - 2X_1X_2 - 228912.661109$
8	$0.627012X_1 + 2243.941710X_2 - 17.958249X_1^{0.5} - 6349.659043X_2^{0.5} - 0.108517\text{E} - 4X_1^2 - 139.828603X_2^2 + 3.022139X_2^3 - 0.251592\text{E} - 1X_2^4 + 0.727708\text{E} - 4X_2^5 - 0.551382\text{E} - 2X_1X_2 - 215177.705695$

Table A.5 – Continued

Hour t	Model
9	$0.725096X_1 + 2290.330344X_2 - 25.352354X_1^{0.5} - 6510.066289X_2^{0.5} - 0.156428\text{E} - 4X_1^2 - 140.824459X_2^2 + 3.043128X_2^3 - 0.254020\text{E} - 1X_2^4 + 0.737832\text{E} - 4X_2^5 - 0.549182\text{E} - 2X_1X_2 - 201021.938579$
10	$0.312872X_1 + 2184.487993X_2 + 0.633035X_1^{0.5} - 6197.468860X_2^{0.5} - 0.178826\text{E} - 5X_1^2 - 136.829709X_2^2 + 2.958440X_2^3 - 0.246099\text{E} - 1X_2^4 + 0.711464\text{E} - 4X_2^5 - 0.534920\text{E} - 2X_1X_2 - 187572.110969$
11	$0.387970X_1 + 2109.643931X_2 - 16.388782X_1^{0.5} - 5873.084358X_2^{0.5} + 0.311075\text{E} - 5X_1^2 - 134.967423X_2^2 + 2.924033X_2^3 - 0.242749\text{E} - 1X_2^4 + 0.698797\text{E} - 4X_2^5 - 0.542021\text{E} - 2X_1X_2 - 173713.869743$
12	$1.205862X_1 + 2274.747239X_2 - 65.508564X_1^{0.5} - 6476.992754X_2^{0.5} - 0.248248\text{E} - 4X_1^2 - 137.306926X_2^2 + 2.942874X_2^3 - 0.243286\text{E} - 1X_2^4 + 0.698062\text{E} - 4X_2^5 - 0.550205\text{E} - 2X_1X_2 - 159764.329280$
13	$0.882523X_1 + 2194.843658X_2 - 28.593420X_1^{0.5} - 6279.211998X_2^{0.5} - 0.209193\text{E} - 4X_1^2 - 133.585958X_2^2 + 2.876141X_2^3 - 0.238682\text{E} - 1X_2^4 + 0.687497\text{E} - 4X_2^5 - 0.536216\text{E} - 2X_1X_2 - 147111.844728$
14	$0.647145X_1 + 2110.029782X_2 - 8.421409X_1^{0.5} - 6101.144024X_2^{0.5} - 0.198360\text{E} - 4X_1^2 - 128.859585X_2^2 + 2.775694X_2^3 - 0.229981\text{E} - 1X_2^4 + 0.660306\text{E} - 4X_2^5 - 0.519247\text{E} - 2X_1X_2 - 133664.219791$
15	$-0.301423X_1 + 1941.095985X_2 + 67.800279X_1^{0.5} - 5665.359802X_2^{0.5} - 0.964160\text{E} - 6X_1^2 - 121.139625X_2^2 + 2.593356X_2^3 - 0.210941\text{E} - 1X_2^4 + 0.587700\text{E} - 4X_2^5 - 0.563212\text{E} - 2X_1X_2 - 121308.344327$
16	$-1.134184X_1 + 1367.401675X_2 + 66.667109X_1^{0.5} - 3556.508729X_2^{0.5} + 0.586959\text{E} - 4X_1^2 - 108.465793X_2^2 + 2.426615X_2^3 - 0.201998\text{E} - 1X_2^4 + 0.576823\text{E} - 4X_2^5 - 0.553373\text{E} - 2X_1X_2 - 108211.800318$

Table A.5 – Continued

Hour t	Model
17	$1.851391X_1+2028.462777X_2-139.993518X_1^{0.5}-5737.643234X_2^{0.5}-0.324398\text{E}-4X_1^2-123.924011X_2^2+2.686386X_2^3-0.225160\text{E}-1X_2^4+0.658439\text{E}-4X_2^5-0.582260\text{E}-2X_1X_2-92601.907255$
18	$1.391922X_1+1858.470716X_2-72.195064X_1^{0.5}-5310.261340X_2^{0.5}-0.248974\text{E}-4X_1^2-115.038811X_2^2+2.503641X_2^3-0.209851\text{E}-1X_2^4+0.613021\text{E}-4X_2^5-0.633896\text{E}-2X_1X_2-82236.626282$
19	$1.132653X_1+1661.184618X_2-39.639640X_1^{0.5}-4778.860098X_2^{0.5}-0.204149\text{E}-4X_1^2-105.246267X_2^2+2.309204X_2^3-0.194407\text{E}-1X_2^4+0.569962\text{E}-4X_2^5-0.631293\text{E}-2X_1X_2-70415.965156$
20	$1.024894X_1+1541.744471X_2-28.595551X_1^{0.5}-4469.304452X_2^{0.5}-0.187822\text{E}-4X_1^2-97.420008X_2^2+2.160203X_2^3-0.184743\text{E}-1X_2^4+0.553031\text{E}-4X_2^5-0.598982\text{E}-2X_1X_2-57874.074753$
21	$1.013258X_1+1291.603774X_2-26.245348X_1^{0.5}-3787.275406X_2^{0.5}-0.199079\text{E}-4X_1^2-84.149975X_2^2+1.896007X_2^3-0.164536\text{E}-1X_2^4+0.501105\text{E}-4X_2^5-0.562704\text{E}-2X_1X_2-45740.259788$
22	$1.127898X_1+1277.472156X_2-33.207077X_1^{0.5}-3851.711699X_2^{0.5}-0.255273\text{E}-4X_1^2-76.417203X_2^2+1.732570X_2^3-0.154423\text{E}-1X_2^4+0.488102\text{E}-4X_2^5-0.530053\text{E}-2X_1X_2-33372.965678$
23	$0.681600X_1+775.028369X_2+8.651342X_1^{0.5}-2356.233890X_2^{0.5}-0.154240\text{E}-4X_1^2-51.799655X_2^2+1.216008X_2^3-0.110384\text{E}-1X_2^4+0.354457\text{E}-4X_2^5-0.491363\text{E}-2X_1X_2-23750.713466$
24	$1.300856X_1+622.991680X_2-42.983476X_1^{0.5}-1856.578705X_2^{0.5}-0.356728\text{E}-4X_1^2-34.556613X_2^2+0.809821X_2^3-0.758148\text{E}-2X_2^4+0.253297\text{E}-4X_2^5-0.504685\text{E}-2X_1X_2-12601.866707$